Fluid Phase Equilibria 442 (2017) 125–139

Contents lists available at ScienceDirect

Fluid Phase Equilibria

journal homepage: www.elsevier.com/locate/fluid

Thermodynamic models to accurately describe the *PVTxy*-behavior of water / carbon dioxide mixtures

Ailo Aasen [a, b, *], Morten Hammer [a], Geir Skaugen [a], Jana P. Jakobsen [a], Øivind Wilhelmsen [a, b]

[a] SINTEF Energy Research, P.O. Box 4671 Sluppen, NO-7465 Trondheim, Norway
[b] Norwegian University of Science and Technology, Department of Energy and Process Engineering, Kolbjørn Hejes v. 1B, NO-7491 Trondheim, Norway

ARTICLE INFO

Article history:
Received 1 November 2016
Received in revised form
6 January 2017
Accepted 10 February 2017
Available online 4 March 2017

Keywords:
Equation of state
Water
Carbon dioxide
Solubility
Density

ABSTRACT

Carbon dioxide/water (CO_2/H_2O) mixtures are of much interest in carbon capture and storage, atmospheric science, in the description of human lungs and in the processing of food and beverages. We present a comprehensive comparison of thermodynamic models for describing their *PVTxy* behavior, i.e. densities and phase compositions. The most accurate experimental data in the temperature range 273–478 K and at pressures below 61 MPa are selected after a critical data evaluation. The most reliable phase equilibrium data are used to fit the binary interaction parameters of a wide range of thermodynamic models: cubic equations of state (EoS) with quadratic/Wong–Sandler/Huron–Vidal mixing rules, CPA, PC-SAFT and PCP-SAFT with different association schemes, and corresponding states models with various reference fluids. We test the predictive ability of the models by comparing to data outside of the region used in the parameter-fit. All of the thermodynamic models are fitted with the same experimental data and compared on the same basis, facilitating a general discussion about their strengths and weaknesses. As a benchmark for the performance of the models, we compare with the performance of two multiparameter EoS: GERG-2008 and EoS-CG. At least three fitting parameters are needed to represent the *PVTxy* behavior of CO_2/H_2O mixtures within an accuracy of 10%. By including a fourth parameter, it is possible to significantly improve the accuracy for phase compositions, where the Peng–Robinson cubic EoS with the Huron–Vidal mixing rule and volume shift gives the best results with an average accuracy of 4.5% and 2.8% for phase compositions and densities respectively. In comparison, the most accurate multiparameter EoS, EoS-CG, exhibits an average accuracy of 8.0% and 0.6% for phase compositions and densities respectively.

1. Introduction

The phase behavior of the binary system carbon dioxide/water (CO_2/H_2O) is complicated, but ubiquitous in nature and of importance to many industrial applications. Examples range from the physics of volcanoes and human lungs, to processing of food and beverages or production of hydrogen and ammonia in the industry.

One emerging application is carbon capture, transport and storage (CCS), for which the two perhaps most important thermodynamic properties are solubilities (equilibrium phase compositions) and densities. Accurate dew point predictions are needed in transport of humid CO_2-rich mixtures, to avoid a sour water-rich liquid phase and subsequent corrosion of pipelines. Accurate density and solubility predictions of the aqueous phase are important when CO_2 is pumped into aquifers for CO_2-storage [1]. Moreover, for the purpose of enhanced oil recovery, the degree of recovery depends strongly on the portion of CO_2 that dissolves in the brine [2]. Due to its importance and complexity, there is a wealth of literature addressing the CO_2/H_2O system, both in terms of modeling and measurements [3–37]. These works all use a different choice of solubility data to fit the models, rarely consider density predictions, and often test only a single model. It is therefore difficult to compare models from different works, because they vary by the temperature-pressure range considered and the data used in the fitting procedure. In this work, we fit a wide variety of thermodynamic models with the same experimental data and

* Corresponding author. Norwegian University of Science and Technology, Department of Energy and Process Engineering, Kolbjørn Hejes v. 1B, NO-7491 Trondheim, Norway.
E-mail address: ailo.aasen@sintef.no (A. Aasen).

http://dx.doi.org/10.1016/j.fluid.2017.02.006

compare them on the same basis. The goal of this work is fourfold:

1 Build on and refine previous data evaluations for solubility and density measurements for the CO_2/H_2O system and extend them with recent measurements.
2 Based on the data evaluation, use the most accurate solubility measurements to fit binary interaction parameters for a wide range of thermodynamic models.
3 Compare and discuss the accuracy of the models with respect to solubility and density.
4 Explore the accuracy of the models when extrapolated to extreme temperatures and pressures.

The CO_2/H_2O system is of type III according to the phase diagram classification of Scott and van Konynenburg [39]. The phase behavior of the system is illustrated in Figs. 1a and b. Fig. 1a shows the two-, three, and four-phase loci in the *TP*-space, and for reference also the saturation curve of pure CO_2. Fig. 1b shows the *Pxy* phase envelope at $T = 288.15$ K. In the fluid region, the salient feature is the vapor-liquid-liquid (VL_1L_2) coexistence curve, located at pressures slightly below the pure CO_2 saturation curve and terminating in an upper critical end point (UCEP). Hydrates can form at temperatures below 283 K at sufficiently high pressures.

For temperatures below the critical temperature of CO_2 at 304 K, and above the freezing point of water at 273 K, there is vapor-liquid equilibrium ($\mathbf{V} + \mathbf{L}_1$ in Fig. 1a) for pressures below the saturation pressure of CO_2 (solid line), and liquid-liquid equilibrium ($\mathbf{L}_1 + \mathbf{L}_2$) at pressures above the vapor-liquid-liquid equilibrium curve (VL_1L_2). The small pressure interval where these two regions coincide exhibit both VLE and LLE, where varying the total composition will give rise to a water-rich liquid ($\mathbf{L}_1$), a CO_2-rich liquid ($\mathbf{L}_2$) and a CO_2-rich vapor ($\mathbf{V}$); Fig. 1b illustrates this.

We will fit the thermodynamic models to phase equilibrium composition measurements in the temperature range 274–478 K and for pressures below 60.8 MPa; this includes the operating conditions relevant for CCS conditioning, transport and storage [40], and excludes regions where reliable data for at least one of the phases are scarce. Solid phases such as hydrates will not be considered since they require additional models, e.g. van der Waals Platteeuw type of hydrate models [3]. However, thermodynamic models that accurately reproduce the fluid phase equilibria data of a particular water mixture, usually also perform well when predicting hydrate equilibria when coupled with a hydrate model [3].

We restrict the discussion to equations of state (EoS) that are capable of modeling all fluid phases with a single consistent model. This is known as the $\phi - \phi$ approach (see e.g. Ref. [41]). The so-called $\gamma - \phi$ approach, where the liquid phase is modeled with an activity coefficient model and the vapor phase is modeled with a conventional EoS like SRK, will not be considered. The $\gamma - \phi$ approach comes with a number of drawbacks such as not being able to predict the shift from VLE to LLE at subcritical pressures, as well as not being able to predict liquid-phase densities.

The work will be structured as follows: We provide in Sec. 2 a description of the thermodynamic models that will be fitted and evaluated, including EoS, α-parameter correlations and mixing rules, association schemes and reference EoS in corresponding state EoS. An explanation of how the parameters are regressed is provided in Sec. 3. We next present the results in Sec. 4, with the data evaluation in Sec. 4.1 and a discussion of the regressed models in Sec. 4.2. Concluding remarks are given in Sec. 5.

2. Thermodynamic models

The thermodynamic models studied in this work comprise variations of cubic EoS, corresponding states EoS, multiparameter EoS, and EoS explicitly modeling association. An overview of the thermodynamic models and how they are connected is given in Fig. 2, and the models are defined in the subsequent text. The figure shows that there are many choices associated with cubic EoS, such as the type of alpha correlations, mixing rules, and incorporation of so-called volume shifts. Further, the dashed lines elucidate that cubic EoS are used as input in many thermodynamic models such as corresponding state (CSP) models and the cubic plus association (CPA) EoS. Multiparameter EoS and Perturbed-Chain Statistical Associating Fluid Theory (PC-SAFT), however, do not use cubic EoS. Use of PC-SAFT and CPA requires choosing an association scheme,

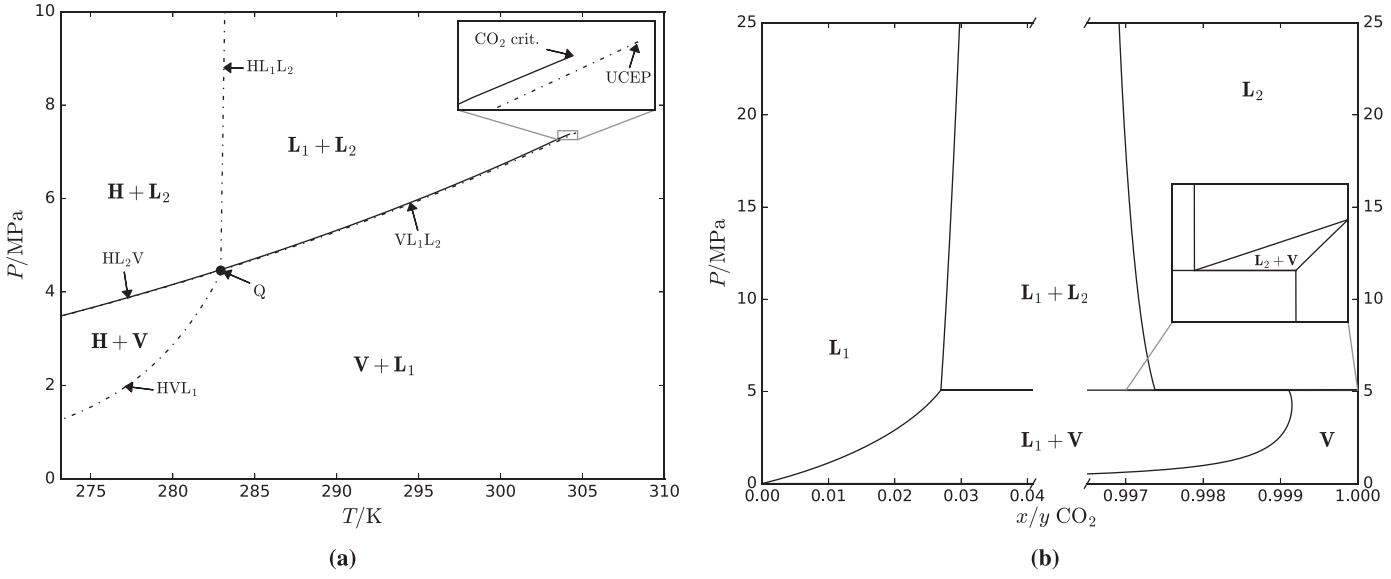

Fig. 1. **(a)** Phase behavior of the CO_2/H_2O system in the temperature-pressure space. Regions of hydrate formation (**H**) can be seen at low temperatures. The solid curve represents the saturation pressure of pure CO_2. Dashed curves: three-phase loci. Q: four-phase point. The correlations used to obtain the coexistence curves are obtained from Refs. [7,38]. **(b)** The *Pxy* phase diagram at $T = 288.15$ K generated by EoS-CG. Inset: scaled diagram of the region between 5.05 and 5.1 MPa with VLE between the two CO_2-rich phases **V** and $\mathbf{L}_2$. The aqueous phase is denoted $\mathbf{L}_1$.

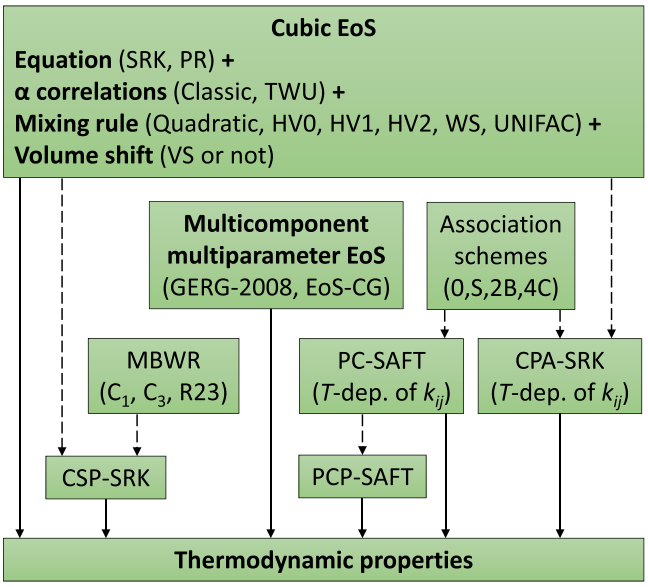

Fig. 2. Overview of models. Dashed arrows signify that one model is used as a building block in another, and names in parentheses represent choices. Each model evaluated in this work corresponds to a certain set of choices in the above diagram. The abbreviations and modeling concepts will be defined in the text.

as well as the temperature-dependence of the interaction parameter k_{ij}, as the figure shows.

2.1. Cubic EoS

The Peng–Robinson EoS (PR) [42] and the Soave–Redlich–Kwong [43] EoS (SRK) are cubic EoS that can be written in pressure-explicit form as

$$P = \frac{RT}{v-b} - \frac{a(T)}{(v+\delta_1 b)(v+\delta_2 b)}, \tag{1}$$

where v is the molar volume, $a(T)$ is the attraction parameter, b is the covolume, and $(\delta_1, \delta_2) = (1+\sqrt{2}, 1-\sqrt{2})$ for PR and $(\delta_1, \delta_2) = (1, 0)$ for SRK.

PR is more accurate in modeling liquid densities than SRK, and the critical compressibility of PR (0.307) is closer to realistic values than that of SRK (0.333); on the other hand, SRK more accurately predicts critical fugacity coefficients [44]. A general method to improve the density predictions of cubic EoS is to use a volume-shift (abbreviated VS), which is simply a composition-dependent shift of the volume; details and correlations for the volume-shift parameters can be found in Refs. [45,46].

2.1.1. The α-correlation

For pure components one has $a(T) = a_0\alpha(T)$, where a_0 and b are chosen to match the critical temperature and pressure (T_c, P_c). The alpha correlation $\alpha(T)$ is a somewhat arbitrary function that is usually chosen so to accurately reproduce the saturation curve, and is either (a) correlated in terms of the acentric factor, or (b) fitted to pure-component saturation pressures and/or liquid densities. Unless otherwise stated, we have used the classic alpha correlation $\alpha(T) = [1 + m(\omega)(1-\sqrt{T_r})]^2$ for the cubic equations, where $T_r = T/T_c$ and the acentric factor-correlation $m(\omega)$ is given in Refs. [42,43]. However, we have also tested the effect of using the more accurate alpha correlation by Twu et al. [47] with three fitted parameters (hereafter abbreviated TWU), given by

$$\alpha(T_r) = T_r^{N(M-1)} \exp\left[L\left(1 - T_r^{MN}\right)\right]. \tag{2}$$

We fitted L, M and N in Eq. (2) to the saturation pressures coming from the reference EoS ([36]) for H_2O and CO_2. The resulting parameters are given in Table 1.

2.1.2. Mixing rules

A mixing rule converts pure-component parameters into mixture parameters, and answers what a and b in Eq. (1) is for a mixture. The mixture covolume is usually calculated as a quadratic sum of binary cross parameters b_{ij},

$$b = \sum_i \sum_j x_i x_j b_{ij}, \quad b_{ij} = \left[\frac{b_i^{1/s} + b_j^{1/s}}{2}\right]^s. \tag{3}$$

A common choice is to set $s = 1$ and let the mixture covolume become a linear combination of the pure fluid covolumes. Unless otherwise stated, we have used $s = 1$. However, most of the available mixing rules are for the attraction parameter a, and we shall next discuss the most common choices.

2.1.2.1. Quadratic mixing rules. The mixture attraction parameter is in the quadratic mixing rule given by

$$a = \sum_i \sum_j x_i x_j a_{ij}, \quad a_{ij} = \sqrt{a_i a_j}(1 - k_{ij}), \tag{4}$$

where k_{ij} is a binary interaction parameter (BIP) fitted to solubility data. This mixing rule is used unless otherwise stated.

Excess Gibbs energy models can be included in cubic EoS as mixing rules by considering the infinite (G^E_∞) or zero (G^E_0) pressure limit [48,49]. The mixture attraction parameter a of the cubic EoS then takes the following form in the infinite pressure limit:

$$\frac{a}{RTb} = \sum_i x_i \frac{a_i}{RTb_i} - \frac{1}{h_\infty}\frac{G^E_\infty}{RT}. \tag{5}$$

Here $h_\infty = \frac{1}{\delta_2 - \delta_1}\ln\frac{1+\delta_2}{1+\delta_1}$, with δ_1 and δ_2 defined in Eq. (1). In the zero pressure limit one uses the following expression for the mixture attraction parameter a:

$$\frac{a}{RTb} = \sum_i x_i \frac{a_i}{RTb_i} - \frac{1}{h_0}\left(\sum_i x_i \ln\frac{b}{b_i} + \frac{G^E_0}{RT}\right), \tag{6}$$

where h_0 equals -0.593 for SRK and -0.53 for PR. A model for G^E_0 or G^E_∞ thus yields one equation for the two mixture parameters a and b, and one additional equation is thus needed for a full mixing rule.

Some of the most common excess Gibbs energy (G^E) mixing rules are the group contribution (GC) methods, e.g. UNIFAC, and the Huron–Vidal or the Non-Random Two-Liquid (NRTL) rule. Also interesting is the Wong–Sandler rule, which has been shown to perform well in the critical region for binary systems of CO_2 with O_2 or N_2 [50,51].

2.1.2.2. UNIFAC mixing rules. The UNIFAC (*UNI*QUAC *F*unctional-

Table 1
TWU parameters fitted to saturation pressures from the triple point up to 301 K (CO_2) and 630 K (H_2O).

α-correlation	CO_2 (L, M, N)	H_2O (L, M, N)
SRK-TWU	(0.046115, 0.91388, 6.8838)	(0.36117, 0.87308, 2.4389)
PR-TWU	(0.022762, 0.92848, 7.7217)	(0.40274, 0.87000, 1.8869)

group Activity Coefficients) model [52] is a GC version of the UNIQUAC model [53]. The underlying idea of GC models is to treat pure species as being composed of functional groups, and then focus on modeling group-group interactions. If the group interaction energies are known from e.g. fits to experimental VLE data, these parameters can be used to predict properties for any molecule comprised of known functional groups. Examples of such groups are CH_2 and CH_3, that can be thought of as monomers in a hydrocarbon polymer. A molecule too small to divide into groups is usually considered a group in itself; in particular, this is the case for both CO_2 and H_2O.

For the original UNIFAC model the overall excess Gibbs energy is the sum of two terms: a combinatorial contribution describing the excess Gibbs energy arising from differences in molecular size and shape, and a residual term describing the excess Gibbs energy differences due to molecular interactions. The UNIFAC residual term, G^R, is in this work used as defined by Fredenslund et al. [52]. Adding the combinatorial term $G^{E,C}$, the overall excess Gibbs energy for the UNIFAC model becomes

$$\frac{G^E}{RT} = \frac{G^R}{RT} + \frac{G^{E,C}}{RT}.$$

The $G^{E,C}$ term is derived from statistical mechanics, and comprises the Flory–Huggins (FH) [54,55] combinatorial and the Staverman–Guggenheim (SG) correction term [56],

$$G^{E,C} = G^{E,FH} + G^{E,SG}.$$

The UNIFAC excess Gibbs mixing rule has found applications in the predictive SRK (PSRK) model [57], and later a volume shifted PR (VTPR) model from the same group [58]. It is also used as the universal mixing rule (UMR) [59] together with translated–modified PR (t-mPR) EoS [60,61]. The combined model is denoted PR-UMR. Both VTPR and PR-UMR make similar changes to improve on the performance of the earlier PSRK model, that gave poor predictions in highly non-symmetric systems, containing both long chain molecules and short chain molecules. VTPR ignores the entire combinatorial term while PR-UMR ignores the Flory–Huggins contribution. VTPR and PR-UMR apply the zero pressure limit when including the excess Gibbs energy in the cubic EoS, Eq. (6), but ignore the logarithmic term. As a consequence, the expression for the attraction parameter a becomes as for the infinite pressure limit, using h_0 instead of h_∞.

VTPR uses modified UNIFAC parameters, and the parameter set used in this work is taken from Schmid et al. [62]. Further, VTPR uses the TWU α-correlation in Eq. (2), and $s = 4/3$ is used in the covolume mixing rule in Eq. (3). PR-UMR uses the original temperature-independent UNIFAC parameters published by Hansen et al. [63] and the Dortmund Data Bank [64]. $s = 2$ is used as covolume mixing parameter in Eq. (3). For simplicity we apply the same volume–shift for both VTPR and PR-UMR, namely a Péneloux type volume-shift adapted for PR [46].

2.1.2.3. Huron–Vidal mixing rules. Huron and Vidal [48] derived an expression for the infinite pressure excess Gibbs energy of cubic EoS, and equated it with a modified NRTL model that contains the quadratic mixing rule Eq. (4) as a special case. The modified NRTL model is given by

$$G^E_\infty = RT\sum_i^{NC} x_i \frac{\sum_j^{NC}\tau_{ji}b_j x_j C_{ji}}{\sum_k^{NC} b_k x_k C_{ki}}, \quad \tau_{ji} = \frac{\Delta g_{ji}}{RT}. \tag{7}$$

Here, $\Delta g_{ji}/R$ is either a zeroth, first, or second order polynomial in temperature

$$\Delta g_{ji}/R = d_{ji} + e_{ji}\cdot T + f_{ji}\cdot T^2,$$

and $C_{ji} = \exp(-\alpha_{ji}\tau_{ji})$. In this work, we have used $\alpha_{ij} = \alpha_{ji} = 0.03$. Indeed, the model in Eq. (7) is insensitive to the value of α_{ij}. Depending on the degree of the polynomial τ_{ji}, the models employ 2, 4 or 6 BIPs, which we will refer to as HV0, HV1, and HV2, respectively, where the number refers to the degree of the polynomial. Huron–Vidal uses linear covolume mixing, i.e. $s = 1$ in Eq. (3); in fact G^E_∞ of cubic EoS diverges unless linear covolume mixing is used.

2.1.2.4. Wong–Sandler (WS) mixing rules. Wong and Sandler [65] derived an expression for the infinite pressure excess Helmholtz energy A^E_∞ of a cubic EoS, and equated it with the NRTL model [66]. The NRTL model for G^E_∞ is given by Eq. (7) with $b_i = 1$, and as in the Huron–Vidal rule we set $\alpha_{ij} = \alpha_{ji} = 0.03$. Combining this G^E_∞ model with Eq. (5) gives one equation for a and b. The second equation enforces a quadratic composition dependence of the second virial coefficient, as is required by statistical mechanics:

$$b - \frac{a}{RT} = \sum_i \sum_j x_i x_j \left(b - \frac{a}{RT}\right)_{ij}, \tag{8}$$

where the combining rule is given in Eq. (9). The Wong–Sandler rule uses the three BIPs k_{ij}, e_{ij} and e_{ji}, given by

$$\Delta g_{ji}/R = e_{ji}\cdot T,$$

and

$$b_{ij} - \frac{a_{ij}}{RT} = \frac{\left(b_i - \frac{a_i}{RT}\right) + \left(b_j - \frac{a_j}{RT}\right)}{2}(1 - k_{ij}). \tag{9}$$

2.2. Corresponding states EoS

The corresponding states approach (here called CSP) is described in detail by Michelsen and Mollerup [44]. The idea behind this approach is to use an accurate EoS for a pure component, and then map any mixture state $(T, v, n_1, \ldots)$ to a state (T_0, v_0) of the pure component; where the hypothesis is that an accurate description of the pure fluid will give an accurate description of any mixture, relying thus on the principle of corresponding state. This modeling approach is associated with three choices: 1) what component to use as the reference fluid, 2) what equation to use for modeling the reference fluid and 3) how to compute the *shape factors* T/T_0 and v/v_0. In this work, we use the SRK EoS to compute the shape factors with conventional α correlations, but we will test both the quadratic and the Huron–Vidal mixing rules.

The CSP approach in conjunction with cubic EoS has been tested in several previous works [67–69], and has shown to improve density predictions in comparison to standard SRK and PR. Another advantage with the CSP approach when using a cubic EoS for the shape factors, is that T_c and P_c are reproduced exactly. This work uses the reference components C1 (methane), C3 (propane) and R23 (fluoroform), all modeled using a modified Benedict–Webb–Rubin (MBWR) multiparameter EoS. These models will be referred to as CSP-SRK-C1, CSP-SRK-C3, CSP-SRK-R23, respectively. Parameters for the MBWR equations can be found in Ref. [70] for C1 and C3, and in Ref. [71] for R23.

2.3. Association theories: CPA and PC-SAFT variants

Association theories explicitly model interactions such as hydrogen bonding (association) by allowing a molecule to have several electron acceptor and/or donor sites, where sites of different polarity interact. The resulting EoS model the Helmholtz energy, A, by adding an association term to some underlying "physical" contribution:

$$A = A^{\text{phys}} + A^{\text{assoc}}. \tag{10}$$

Within the association theories, we will in this work evaluate CPA-SRK [72] (using $A^{\text{phys}} = A^{\text{SRK}}$), PC-SAFT [73] and PCP-SAFT [74–76]; more specifically, we use the versions of them that employ the simplified mixing rules described in Refs. [77,78]. Since several, slightly different forms of the A^{assoc} term exist in the literature, we explicate the association contribution:

$$A^{\text{assoc}} = RT\sum_i n_i \sum_{A_i}\left(\ln X_{A_i} - \frac{X_{A_i}}{2} + \frac{1}{2}\right),$$

where R is the gas constant, the n_i are mole numbers, and X_{A_i} is the fraction of molecules *not* bonded at site A_i in molecule i. X_{A_i} is given by the implicit equation

$$1/X_{A_i} = 1 + (1/V)\sum_j n_j \sum_{B_j} X_{B_j}\Delta^{A_iB_j}.$$

Here $\Delta^{A_iB_j}$ is the bond association strength, and is given by

$$\Delta^{A_iB_j} = g_{ij}\phi_{ij}\kappa^{A_iB_j}\left[\exp\left(\varepsilon^{A_iB_j}\Big/RT\right) - 1\right],$$

where ϕ_{ij}, $\kappa^{A_iB_j}$, $\varepsilon^{A_iB_j}$ are binary parameters obtained from pure-component parameters using combining rules. ϕ_{ij} and the radial distribution function g_{ij} differ between PC-SAFT and CPA. For PC-SAFT they are given by

$$g_{ij} = \frac{1-\eta/2}{(1-\eta)^3}, \quad \eta = \frac{\pi}{6}\rho\sum_i x_i m_i d_i^3,$$
$$d_i = \sigma_i\left[1 - 0.12\exp\left(-3\frac{\varepsilon_i}{RT}\right)\right], \quad \phi_{ij} = N_A\left((\sigma_i+\sigma_j)/2\right)^3$$

where N_A is Avogadro's constant, ρ is the density, the x_i are mol-fractions, while m_i, σ_i and ε_i are pure-component parameters for PC-SAFT. For CPA-SRK g_{ij} and ϕ_{ij} are given by

$$g_{ij} = \frac{1-y/2}{(1-y)^3}, \quad y = b\rho/4, \quad \phi_{ij} = \frac{b_i+b_j}{2}$$

where b is the mixture covolume, and b_i, b_j are the pure-component covolumes of the SRK EoS, cf. Eq. (1). We will follow convention and assume that all acceptor and donor sites within a molecule are identical, and if we wish we can thus simplify notation as follows: $\Delta^{A_iB_j} \mapsto \Delta^{ij}$, $\varepsilon^{A_iB_j} \mapsto \varepsilon^{ij}$, $\kappa^{A_iB_j} \mapsto \kappa^{ij}$.

Popular choices of association schemes for molecules are the 2B scheme (1 donor and 1 acceptor), the 4C scheme (2 donors and 2 acceptors), and the trivial 0 association scheme (0 donors and acceptors) where the molecule does not take part in association. Several different association schemes for the CO_2/H_2O system have been tested for association models, but what the optimal scheme is remains unclear. From a physical perspective, water is dipolar while carbon dioxide is non-dipolar but with a large quadrupole moment. Ab initio calculations by Danten et al. [79] indicate that the resulting forces induce effects akin to a weak hydrogen-bonding between H_2O and CO_2, in which CO_2 acts as the electron acceptor. Tsivintzelis et al. [80] thus tested a model of CO_2 which excluded self-association but allowed cross-association, with CO_2 having either one or two electron acceptor sites; this is called *solvation*. We have included a comparable model (CPA-SRK-S4C), where the CO_2 molecule has 1 electron acceptor but no donors, so that it does not self-associate but cross-associates with the electron donors on H_2O. We will refer to this as the S association scheme.

2.3.1. CPA-SRK

The CPA-SRK EoS was developed by Kontogeorgis et al. [72] by adding an association term to SRK. This work uses the CPA-SRK model with the simplified mixing rules described in Kontogeorgis et al. [77] (simplified CPA). CPA-SRK has previously been evaluated for the CO_2/H_2O system [80]. The counterpart CPA-PR is also in active use [81].

The pure-component parameters are provided in Table 2. Since no parameters were found in the literature using the 2B scheme for H_2O, they have been fitted as part of this work and are listed in Table 2. The binary parameter we have fitted for CPA-SRK is k_{ij} in the quadratic mixing rule of the SRK EoS, cf. Eq. (4). For the solvation model CPA-SRK-S4C we have also fitted the association energy ε_1 and association volume κ_1 of CO_2 with 1 acceptor and 0 donors; these are listed in Table 5.

2.3.2. PC-SAFT

This work evaluates the simplified PC-SAFT proposed by von Solms et al. [78]. For pure components it has the same form as the original PC-SAFT by Gross and Sadowski [73], but uses simplified mixing rules for the radial distribution function and hard-sphere terms; it has in all considered cases been found to have accuracy comparable to the original PC-SAFT. PC-SAFT models A^{phys} as

$$A^{\text{phys}} = A^{\text{ideal}} + A^{\text{hard-chain}} + A^{\text{disp}}.$$

There are three pure-component parameters for non-associating components, namely the number of segments m, the well-depth ε, and the molecular diameter σ. Associating components also have nonzero association energy $\varepsilon^{A_iB_j}$ and association volume $\kappa^{A_iB_j}$ between site A_i on molecule i and site B_j on molecule j. The PC-SAFT pure-component parameters for CO_2 modeled as non-associating are taken from Ref. [73]; H_2O 2B parameters are from Ref. [82]; H_2O 4C parameters are from Ref. [41].

For PC-SAFT we use the conventional combining rules

Table 2
Pure-component parameters used for CPA-SRK. The 2B scheme for H_2O was fitted against reference data [36] saturation pressures and liquid volumes between 273 K up to 630 K.

Component	Scheme	a[m^{6}Pa/mol^2]	b[m^3/mol]	c[−]	ε[J/mol]	κ[−]	Ref.
CO_2	0	0.35079	2.72E-5	0.7602	0	0	[41]
H_2O	2B	0.46754	1.5798E-5	0.77667	4449.53	6.2192E-3	This work
H_2O	4C	0.12277	1.4515E-5	0.67359	16655	69.2E-3	[41]

$$\sigma_{ij} = (\sigma_i + \sigma_j)/2, \quad \varepsilon_{ij} = \sqrt{\varepsilon_i \varepsilon_j}(1 - k_{ij}),$$

$$\varepsilon^{A_iB_j} = \left(\varepsilon^{A_iB_i} + \varepsilon^{A_jB_j}\right)\Big/2,$$

$$\kappa^{A_iB_j} = \sqrt{\kappa^{A_iB_i}\kappa^{A_jB_j}}\left(\sqrt{\sigma_i\sigma_j}\Big/\sigma_{ij}\right)^3.$$

The BIP k_{ij} is the fitting parameter of the PC-SAFT models, and it can be constant, or incorporate a temperature-dependence using a first (ORD1) or second (ORD2) order polynomial in T: $k_{ij}(T) = A + B{\cdot}T + C{\cdot}T^2$.

2.3.3. PCP-SAFT

The PCP-SAFT model [74–76] extends PC-SAFT by explicitly modeling Helmholtz energy contributions due to dipole-dipole (DD), quadrupole-quadrupole (QQ), and dipole-quadrupole (DQ) interactions:

$$A^{\text{phys}} = A^{\text{ideal}} + A^{\text{hard-chain}} + A^{\text{disp}} + A^{\text{QQ}} + A^{\text{DD}} + A^{\text{DQ}}. \tag{11}$$

We will model the quadrupole moment of CO_2, and follow the convention [74,83] of ignoring the dipole and quadrupole moment of H_2O, hoping that contributions from these moments are effectively subsumed in the association contribution A^{assoc}. Thus for the CO_2/H_2O system the last two terms of Eq. (11) are zero, while A^{QQ} models the interaction between quadrupoles of CO_2-molecules. One new pure-component parameter enters in A^{QQ}, namely the quadrupole moment of CO_2; we have used the pure-component parameters from Ref. [74], where the quadrupole moment is not fitted but taken from measurements.

The underlying PC-SAFT EoS used in PCP-SAFT is the one with the simplified mixing rules; we later present evidence that this simplification does not significantly alter the aggregate PCP-SAFT model. The fitting parameter for PCP-SAFT is the k_{ij} of PC-SAFT.

2.4. Multicomponent, multiparameter EoS

The components CO_2 and H_2O are included in both GERG-2008 [84] and its recent variant, the equation of state for combustion gases (EoS-CG) [36]. These multicomponent, multiparameter equations have model forms allowing them to fit all available high-accuracy thermodynamic data (including phase compositions, density, heat capacity, speed of sound), with an error approaching experimental uncertainties. EoS-CG was developed with specific focus on humid gases and CCS mixtures, and is an improvement of the GERG-2008 model for six components, two of which are H_2O and CO_2. Multiparameter EoS are superior when it comes to reproducing experimental data, but are computationally demanding, not easily extended to new components, and require a lot of work to fit. Having many parameters compared to simpler models, the process of fitting multiparameter EoS demands an understanding of the uncertainty in the data to avoid modeling the random noise of measurements. We will however not refit these models, but use the original parameters [36,84].

3. Model regression procedure

To obtain the parameters of the various the mixing rules for the attraction parameter, a, the following objective function was minimized:

$$S = \sum_{i=1}^{m}\left|\frac{x_i^{\text{measured}} - x_i^{\text{model}}}{x_i^{\text{measured}}}\right| + \sum_{j=1}^{n}\left|\frac{y_j^{\text{measured}} - y_j^{\text{model}}}{y_j^{\text{measured}}}\right|, \tag{12}$$

where x_i $(i = 1, \ldots m)$ represent the molefractions of CO_2 in the aqueous phase, and y_j $(j = 1, \ldots n)$ represent the molefractions of H_2O in the CO_2-rich phase. Further, S is a scaled total average absolute deviation (AAD), with the total AAD being $S/(n+m)$. Scaling the deviations by the molefractions as in Eq. (12) does not take into account that some of the data have lower uncertainty than others. Scaling by the measurement standard deviations would rectify this; however, these are not always reliable and often not reported.

The objective function in Eq. (12) does not penalize errors in pressure or density, which is possible by using orthogonal distance regression [85]. This is justified for the CO_2/H_2O system, since the pressure dependence of the solubility is very modest (i.e. nearly vertical *Pxy* envelopes), and since the low mutual solubilities make computed densities insensitive to the parameters in the EoS mixing rule.

Often, a sum of *squared* errors is minimized in the fitting process, even though the AAD is used for reporting the results. One advantage of using squared errors is that it gives a differentiable objective function, allowing for gradient optimization methods. In our experience, however, non-gradient methods such as Nelder-Mead (as used in this work) are adequate. Another argument for using squared errors is that large errors are highly weighted in the sum; however, this has the potential drawback of giving extreme weights to data points where the measured molefraction is very close to zero.

We emphasize that any reasonable choice of objective function in Eq. (12) will likely lead to the same qualitative conclusions of the model comparison drawn in this work.

4. Results and discussion

In Sec. 4.1 we conduct a critical evaluation of the available experimental data. Here, the most accurate solubility data are identified, which extends and refines previous work on the topic [6–9]. The most accurate solubility data are next used to regress the binary interaction parameters of the thermodynamic models presented in Sec. 2, using the methodology described in Sec. 3. The resulting thermodynamic models are evaluated and compared in Sec. 4.2.

4.1. Data evaluation

As an initial part of this work, we performed a survey of solubility and density measurements for the CO_2/H_2O system available in the literature. We only surveyed fluid phase data, and point the reader interested in hydrates to other recent experimental and modeling works [3,4]. We limit the domain of the literature survey to temperatures in the range 274–478 K and pressures below 60.8 MPa, both to cover the entire domain for CCS operating conditions [40], and to avoid regions where reliable measurements are scarce. We found that measurements are generally scarcer at higher temperatures and pressures.

4.1.1. Solubility measurements

There are many formal methods for evaluating the thermodynamic "consistency" of VLE/LLE measurements. They are usually based on thermodynamic identities coupled with some approximations (see e.g. Ref. [5]). For the CO_2/H_2O system, the following criteria were used to evaluate the experimental data:

1 The agreement between data from different publications.
2 The judgment of previous data evaluations [6–10].
3 The agreement between different publications.
4 The agreement with models.

Exhaustive data evaluations and $\gamma - \phi$-like solubility correlations of fluid phase compositions were made by Diamond and Akinfiev (2003) [7] for the aqueous phase, Duan and Sun (2003) [10] for the aqueous phase, and Spycher et al. (2003) [6] for all phases. The latter work focuses on the CO_2-rich phase, up to 373 K and 600 bar. Notable experimental works published after these surveys are [8,11–22]; these do not include measurements limited to very low pressures, to hydrate conditions, or that only comprise a small number of measurements taken to validate experimental setups.

4.1.1.1. Questionable measurements. The much cited works by Takenouchi and Kennedy (1964) [86] and Tödheide and Franck (1963) [87] have dew point measurements that are inconsistent with the remaining bulk of experimental data [6,8,9]. Moreover, we deem the bubble point measurements by Guo et al. (2014) [20] more accurate than those in Refs. [86,87], and therefore use none of the data in Refs. [86,87] in the fitting process.

The measurements by Gillespie and Wilson (1982) [88] have been questioned by several data surveys. Meyer and Harvey (2015) [19] used their dew point data to estimate the second cross virial coefficient B_{12} for the CO_2-rich phase, and found an erratic temperature-dependence. Spycher et al. [6] remarked that several of their measurements fell "off-trend", while Diamond and Akinfiev [7] assigned their bubble point data a confidence factor of zero. We have therefore excluded the data by Gillespie and Wilson from the fitting process.

In the LLE region, the measurements by Hou et al. (2013) [16] are inconsistent with the rest of the data. Their 6 strongly deviating LLE measurements (cf. Fig. 3a) are not used in the fitting process. None of our models are able to reproduce the trend in their LLE data, and in their own paper, they only employ $\gamma - \phi$ models to correlate their VLE data, not their LLE data. Their VLE data however, seem to be of very high quality, consistent with most models in this paper as well as the remaining bulk of the experimental data. We only used the VLE data of Ref. [16] in the fitting process.

With the addition of new data [16,20] for the aqueous phase, there is strong indication (see Fig. 3) that the measurements by Wiebe and Gaddy [23,24] underestimate the CO_2 solubility. Moreover, the models generally fit these measurements poorly, even though they can be well-fitted to data by Hou et al. (2013) 16 and Guo et al. (2014) [20] in the same *TP*-range. Our conclusion contrasts the fact that previous surveys have rated the data in Refs. [23,24] as reliable, with Diamond and Akinfiev [7] even assigning them the highest confidence factor; still, we exclude all data from Refs. [23,24].

Valtz et al. [11] measured compositions of both the aqueous and the CO_2-rich phases in the range of 278.22–318.23 K and 0.47–7.96 MPa. We have excluded Valtz et al.'s dew point data in the fitting, since the dew data by Meyer and Harvey [19] cover the same region, are better reproduced by models, and have better inherent consistency [19]. We will however use Valtz et al.'s aqueous phase data.

4.1.1.2. Overview of accepted measurements. An overview of the experimental data used in this work is given in Table 3 and illustrated in the temperature-pressure space in Fig. 4. Notice the paucity of reliable high-pressure vapor phase measurements. Most of the high-pressure liquid phase measurements come from Guo et al. (2014) [20], whose measurements show good agreement with other works at low pressures, show little scatter and are well-reproduced by models (e.g. PR-HV1-TWU).

4.1.1.3. Summary of the solubility survey. The conclusions of the data survey for phase compositions are summarized as follows:

- **Aqueous phase.** Equilibrium compositions at pressures below 20 MPa have been thoroughly studied, with measurements from a large number of works being consistent. At higher pressures, we have fitted to the measurements by Guo et al. [20]. This phase has the best data coverage.
- **Vapor phase.** With the recent contribution by Meyer and Harvey [19], the composition is known to a high accuracy up to 353 K and 5 MPa. Other works have larger uncertainty. There are considerable experimental gaps at pressures above 20 MPa.

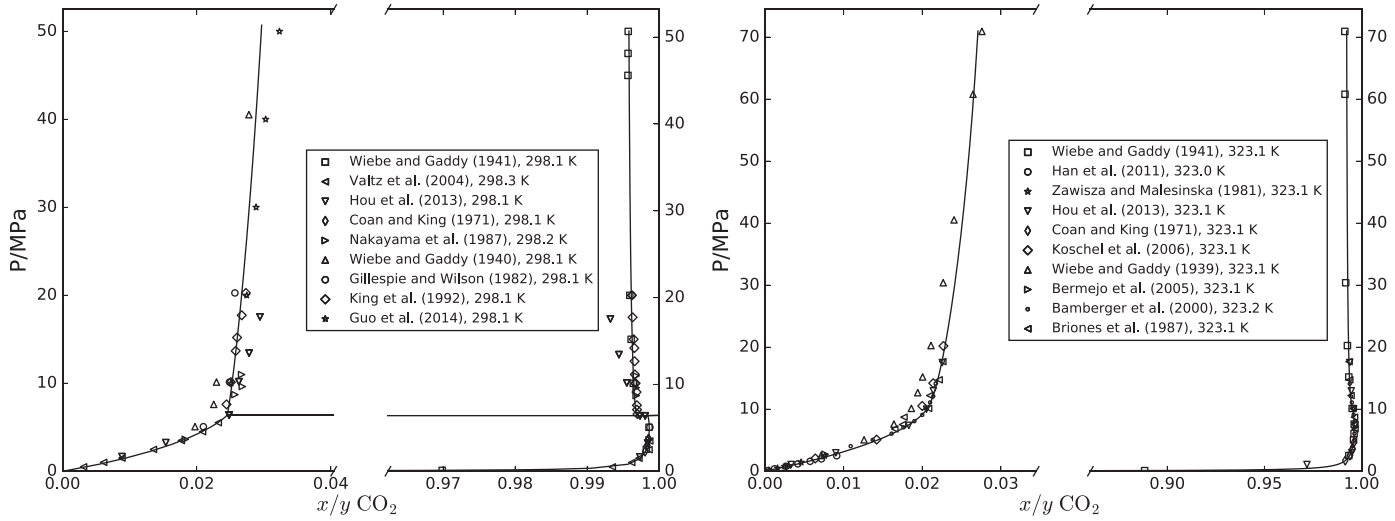

(a) T=298.1 K **(b)** T=323 K

Fig. 3. Measurements (markers) and the phase envelopes calculated by EoS-CG (solid lines) at 298.1 K **(a)** and 323 K **(b)** showing accepted measurements. Some measurements not used in the fitting process are also shown: the aqueous phase data by Wiebe and Gaddy [23,24], the LLE data by Hou et al. [16], and the data by Gillespie and Wilson [88].

Table 3
Measurements used for fitting. *N* is the number of phase composition measurements. All measurements by the publication in the stated *TP*-range have been used. L_1 is the aqueous phase, L_2 is the CO_2-rich liquid phase, *V* is the vapor phase.

Publication	*T*-range (K)	*P*-range (MPa)	*N*	Phases
Wiebe and Gaddy (1941) [25]	298.15 – 348.15	0.10 – 60.80	37	L_2/V
Coan and King (1971) [26]	298.14 – 373.07	1.73 – 5.15	22	V
Zawisza and Malesinska (1981) [27]	323.15 – 473.15	0.15 – 5.39	47	L_1/V
Nakayama et al. (1987) [28]	298.19	3.63 – 10.99	8	L_1/L_2
Briones et al. (1987) [29]	323.14	6.82 – 17.68	14	L_1/V
Müller al. (1988) [30]	373.12 – 473.11	0.33 – 7.80	84	L_1/V
King et al. (1992) [31]	288.15 – 313.15	5.17 – 24.32	68	L_1/L_2
Bamberger et al. (2000) [32]	323.20 – 353.10	4.05 – 14.11	58	L_1/V
Anderson (2002) [33]	274.15 – 288.15	0.08 – 2.18	54	L_1
Valtz et al. (2004) [11]	278.22 – 318.23	0.47 – 7.96	47	L_1
Koschel et al. (2006) [13]	323.10 – 373.10	2.06 – 20.20	8	L_1/V
Tabasinejad et al. (2011) [8]	422.98 – 478.35	3.85 – 43.48	28	V
Han et al. (2011) [14]	313.00 – 333.00	0.10 – 2.50	17	L_1
Hou et al. (2013) [16]	298.15 – 448.15	1.09 – 17.46	78	L_1/V
Guo et al. (2014) [20]	288.15 – 473.15	10.00 – 60.00	65	L_1
Meyer and Harvey (2015) [19]	283.15 – 353.15	0.50 – 5.01	58	V

- **CO_2-rich liquid phase.** There is a need for accurate LLE measurements, primarily at temperatures below 298 K. The most recent measurements of this phase at 298.15 K [16] should be checked, since they are highly inconsistent with older experimental works found in the literature [31,88].

4.1.2. Density measurements

4.1.2.1. Aqueous phase. Recently, Hu et al. (2016) [34] evaluated density data for the CO_2/H_2O system, and performed measurements to close some of the gaps. They also presented a density correlation for the *apparent molar volume* v_{Φ,CO_2} of CO_2, a mixture property defined by:

$$v = x_{H_2O} \cdot v_{H_2O}^{\text{pure}} + x_{CO_2} \cdot v_{\Phi,CO_2}.$$

Although v_{Φ,CO_2} depends on temperature and pressure, it is effectively independent of the CO_2 concentration. The density model reproduces all reliable density measurements within 0.45%, and is claimed to be valid in the fluid phase region from 273.15 K to 573.15 K and pressures up to 120 MPa. Hu et al.'s correlation results were used as a reference for the accuracy evaluation of the aqueous phase density predictions by the thermodynamic models explored in this study.

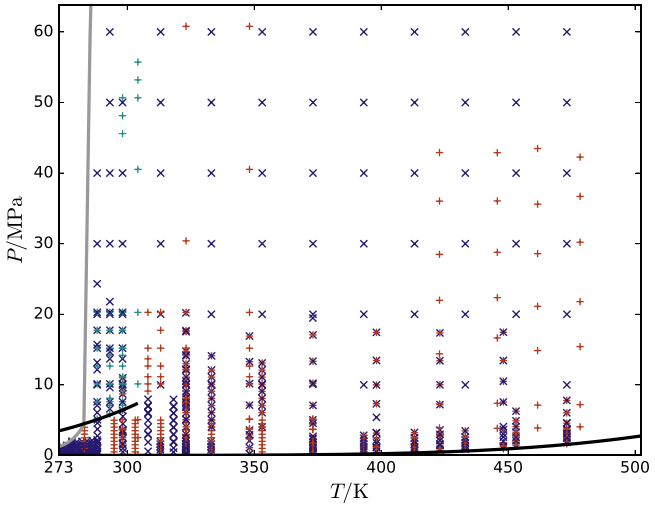

Fig. 4. The measurements used for fitting illustrated in *TP*-space. Symbols: + vapor phase × **V**; aqueous liquid phase **L_1**; + CO_2-rich liquid phase **L_2**. Black curve: pure-component saturation curves. Gray curve: hydrate formation boundary.

4.1.2.2. CO_2-rich phase. We use the EoS-CG model as the benchmark for density predictions of the CO_2-rich phases, since it reproduces all measurements almost within the experimental accuracy [36]. The most reliable density data can be found in the temperature range 323–619 K and for pressures up to 16.4 MPa; they are reproduced within 0.2% by EoS-CG [36]. Below 333 K and between 10 and 300 bar, the CO_2-rich phases have densities essentially equal to the density of pure CO_2 [37]; EoS-CG reproduces the pure-component densities within the experimental uncertainty. However, accurate measurements of the density of the CO_2-rich phases above 16.4 MPa should be performed.

4.2. Evaluation of regressed thermodynamic models in predicting the PVTxy behavior of the CO_2/H_2O mixture

Using the most accurate solubility data identified in Sec. 4.1, we have fitted the mixing rules of several EoS with the total number of fitting parameters varying from one to four. The data used in the fitting process as well as their temperature and pressure ranges are provided in Table 3. In all cases, we used the methodology elaborated in Sec. 3.

4.2.1. The thermodynamic model evaluation

The fitted parameters as well as the performance of the resulting models are presented in Table 5. To ease the readability of Table 5, abbreviations are repeated and explained in Table 4. To gauge the performance of the models in predicting the densities, we compared the models to EoS-CG for the CO_2-rich phase (ρ_y), and Hu et al.'s correlation for the aqueous phase (ρ_x). Densities for both phases were evaluated in the temperature range 283–473 K in intervals of 10 K and at the pressures 0.5, 1, 5, 10, 20, 30, 40, 50 MPa. The densities were computed using the saturation composition as determined from EoS-CG at these *TP*-values, and not the saturation composition as determined by each individual model.

While the solubility predictions depend strongly on the mixing rule, this is not the case for the density predictions, cf. Table 5. This is a result of the low mutual solubilities in the CO_2/H_2O -mixture, causing the densities of the H_2O -rich and the CO_2-rich phases to be close to those of pure H_2O and CO_2, respectively.

We note that all the models that have been studied in this work accurately reproduce the VLLE curve in *TP*-space. This is because all the models detect VLLE very close to the saturation curve of pure CO_2, and all models reproduce the saturation curves within a

Table 4
Explanation of abbreviations used in Table 5.

Abbreviation	EoS (reference comp./assoc. schemes)	Mixing rule (Nr. of par.)	α-correlation
PR-UMR	PR	UNIFAC	Classic
VTPR	PR+volume shift	UNIFAC	Classic
SRK	SRK	Quadratic (1)	Classic
PR	PR	Quadratic (1)	Classic
CSP-SRK-C_1	CSPSRK (C_1)	Quadratic (1)	Classic
CSP-SRK-C_3	CSP+SRK (C_3)	Quadratic (1)	Classic
CSP-SRK-R23	CSP+SRK (R23)	Quadratic (1)	Classic
PC-SAFT-02B	PC-SAFT (CO_2:0, H_2O:2B)	Simpl. PC-SAFT (1)	–
PC-SAFT-04C	PC-SAFT (CO_2:0, H_2O:4C)	Simpl. PC-SAFT (1)	–
CPA-SRK-04C	CPA-SRK (CO_2:0, H_2O:4C)	Simpl. CPA (1)	Classic
CPA SRK-02B	CPA-SRK (CO_2:0, H_2O:2B)	Simpl. CPA (1)	Classic
PR-HV0	PR	Huron–Vidal (2)	Classic
PC-SAFT-02B-ORD1	PC-SAFT (CO_2:0, H_2O:2B)	Simpl. PC-SAFT (2)	–
CPA-04C-ORD1	CPA+SRK (CO_2:0, H_2O:4C)	Simpl. CPA (2)	Classic
PR-WS-TWU	PR	Wong–Sandler (3)	TWU
SRK-WS-TWU	SRK	Wong–Sandler (3)	TWU
PC-SAFT-02B-ORD2	PC-SAFT (CO_2:0, H_2O:2B)	Simpl. PC-SAFT (3)	–
PCP-SAFT-02B	PC-SAFT+A^{QQ}_{CO2} (CO_2:0, H_2O:2B)	Simpl. PC-SAFT (3)	–
CPA-SRK-04C-ORD2	CPA-SRK (CO_2:0, H_2O:4C)	Simpl. CPA (3)	Classic
CPA-SRK-S4C	CPA-SRK (CO_2:S, H_2O:4C)	Simpl. CPA (3)	Classic
CSP-SRK-C1-HV1	CSP+SRK (C_1)	Huron–Vidal (4)	Classic
CSP-SRK-C3-HV1	CSP+SRK (C_3)	Huron–Vidal (4)	Classic
CSP-SRK-R23-HV1	CSP+SRK (R23)	Huron–Vidal (4)	Classic
SRK-HV1-TWU-VS	SRK+volume shift	Huron–Vidal (4)	TWU
PR-HV1	PR	Huron–Vidal (4)	Classic
PR-HV1-TWU	PR	Huron–Vidal (4)	TWU
PR-HV1-TWU-VS	PR + volume shift	Huron–Vidal (4)	TWU

couple of percent. In other words, any model that is able to accurately fit the saturation pressure of CO_2 seems to also reproduce the VLLE curve well.

In Fig. 5 we have illustrated the best solubility fits we obtained using one, two, three and four fitting parameters, respectively. The figure highlights that two types of thermodynamic models give generally more accurate solubility predictions for the CO_2/H_2O mixture; PC-SAFT using the 2B scheme for water and 0 for CO_2, and cubic EoS with Huron–Vidal mixing rules. We next discuss the results for each EoS, highlighting their strengths and weaknesses.

4.2.1.1. Cubic EoS and multiparameter EoS. Table 5 and Fig. 5 highlight the remarkable ability of simple cubic EoS to accurately reproduce even complex phase behavior if the right mixing rule is applied. This is in line with results from e.g. Austegard et al. [89], but unlike them we find that the extra fitting parameters in the PR-HV2-TWU model (6 parameters) do not significantly lower the solubility AAD beyond what PR-HV1-TWU (4 parameters) offers. A comparison of PR-HV1 and PR-HV1-TWU in Table 5 shows that the effect of using the more accurate TWU alpha correlation is to decrease the solubility AAD for the CO_2-rich phase by 3 percentage points. Although the liquid-phase density predictions from standard cubic EoS are generally poor, a simple volume shift greatly ameliorates this for the aqueous phase, at the slight expense of the CO_2-rich phase density.

It is remarkable that the PR-HV1-TWU model, with only four fitting parameters, exhibits a lower total solubility AAD (4.5%) than the very recently fitted multiparameter EoS-CG (8.0%). However, it must be emphasized that EoS-CG was not fitted directly to the data chosen in this work, and was fitted to more properties than just phase compositions and densities. Moreover, it is clear from Table 5 that GERG-2008 has not been fitted to aqueous phase compositions. However, the two multiparameter EoS predict densities more accurately than the other models.

4.2.1.2. Group contribution approaches. Table 5 shows that the two group contribution EoS PR-UMR and VTPR are more accurate than the standard cubic EoS in terms of the total solubility AAD, even though the latter were equipped with one interaction parameter fitted directly to the data. In particular, the VTPR model displays a total solubility AAD of 26.0%, which is less than half of the AAD of SRK (53.0%) and PR (52.3%). This means that the group contribution parameters that have been fitted in VTPR and PR-UMR capture some of the nonideality in the CO_2/H_2O system. However, similar to multiparameter EoS, group contribution EoS require that high-quality data have been used in the initial fit. When fitting GC models, the parameters for a group must be fitted to data for several components containing that group, and the effects must be de-coupled from the effects of other groups in those components. The reliance on high-quality experimental data, combined with the amount of work needed for fitting, are among the main drawbacks for this type of model.

4.2.1.3. Corresponding states models. Corresponding states (CSP) models are capable of achieving the same accuracy as cubic EoS for the solubility, while generally improving density predictions compared to cubic EoS without volume shift. Using the TWU alpha corelation and volume shift for the CSP models will likely bring the solubility and density AADs down to that of PR-HV1-TWU-VS. We observe that using methane (C1) as reference component in the CSP model gives the most accurate solubility predictions, but using fluoroform (R23) gives the best density predictions. The best reference component therefore varies with the thermodynamic property sought, which is a drawback of the CSP modeling approach.

4.2.1.4. Association EoS. Association EoS are able to accurately fit the solubility data, with the PC-SAFT-02B model being the most accurate SAFT model in terms of solubilities. However, they come at the price of increased computational time and complexity compared to cubic EoS. Moreover, the temperature-dependence of the interaction parameter in the SAFT models used in this paper must be improvised, where we have used a constant, linear or quadratic polynomial. This is in contrast to cubic EoS, where e.g. the

Table 5
AADs and interaction parameters for the models fitted to the data in Table 3. The x column lists AADs for solubility of CO_2 in H_2O, while the ρ_x column gives the AADs for aqueous phase densities; analogously, y signifies the CO_2-rich phase. The columns entitled "Total" give the total AAD over all phases. In the Huron–Vidal and Wong–Sandler mixing rules, index 1 is CO_2 and 2 is H_2O. We have introduced the reference temperature $T_0 = 1000$ K to get adimensional interaction parameters.

Model	x	y	Total	ρ_x	ρ_y	Total	Interaction parameters
Zero fitted interaction parameters							
PR-UMR	63.8	17.7	42.5	3.5	2.3	2.9	–
VTPR	10.7	43.8	26.0	3.3	3.3	3.3	–
One fitted interaction parameter							
SRK	88.6	11.6	53.0	25.7	4.6	15.2	$k_{12} = 0.1513$
PR	89.9	8.7	52.3	16.3	1.6	9.0	$k_{12} = 0.1697$
CSP-SRK-C1	89.7	7.0	51.4	25.7	2.5	14.1	$k_{12} = 0.1909$
CSP-SRK-C3	89.2	10.0	52.5	21.4	0.9	11.2	$k_{12} = 0.1673$
CSP-SRK-R23	89.4	7.9	51.7	12.3	3.1	7.7	$k_{12} = 0.1827$
PC-SAFT-02B	23.8	10.2	17.5	7.8	1.3	4.5	$k_{12} = -0.005927$
PC-SAFT-04C	17.8	30.9	23.9	0.7	1.2	1.0	$k_{12} = -0.03646$
CPA-SRK-04C	15.8	35.3	24.9	0.8	2.4	1.6	$k_{12} = -0.004900$
CPA-SRK-02B	97.2	6.1	55.0	0.9	1.7	1.3	$k_{12} = 0.1383$
Two fitted interaction parameters							
PR-HV0	9.8	12.7	11.1	16.3	1.8	9.0	$\frac{g_{12}}{RT_0} = 4.669,\ \frac{g_{21}}{RT_0} = -3.130$
PC-SAFT-02B-ORD1	12.8	8.5	10.8	7.8	1.2	4.5	$k_{12} = -0.09262 + 0.2529\left(\frac{T}{T_0}\right)$
CPA-SRK-04C-ORD1	10.2	35.5	21.9	0.8	2.5	1.6	$k_{12} = -0.1346 + 0.3987\left(\frac{T}{T_0}\right)$
Three fitted interaction parameters							
PR-WS-TWU	15.1	7.5	11.6	15.9	2.8	9.3	$\left[k_{12}, \frac{g_{12}}{RT_0}, \frac{g_{21}}{RT_0}\right] = \left[0.2905, 12.27\left(\frac{T}{T_0}\right), -5.421\left(\frac{T}{T_0}\right)\right]$
SRK-WS-TWU	16.2	7.9	12.4	25.4	6.3	15.8	$\left[k_{12}, \frac{g_{12}}{RT_0}, \frac{g_{21}}{RT_0}\right] = \left[0.2992, 12.24\left(\frac{T}{T_0}\right), -5.391\left(\frac{T}{T_0}\right)\right]$
PC-SAFT-02B-ORD2	8.3	8.8	8.6	7.8	1.2	4.5	$k_{12} = -0.3990 + 1.988\left(\frac{T}{T_0}\right) - 2.404\left(\frac{T}{T_0}\right)^2$
PCP-SAFT-02B-ORD2	8.9	10.2	9.5	7.8	1.3	4.6	$k_{12} = -0.5363 + 2.221\left(\frac{T}{T_0}\right) - 2.474\left(\frac{T}{T_0}\right)^2$
CPA-SRK-04C-ORD2	10.2	35.5	21.9	0.8	2.5	1.6	$k_{12} = -0.1401 + 0.4143\left(\frac{T}{T_0}\right) - 0.00277\left(\frac{T}{T_0}\right)^2$
CPA-SRK-S4C	9.7	14.2	11.8	0.8	2.2	1.5	$[k_{12}, \epsilon_1/(RT_0), \kappa_1] = [0.08831, 2.595, 5.687 \cdot 10^{-5}]$
Four fitted interaction parameters							
CSP-SRK-C1-HV1	3.8	7.6	5.6	25.6	2.7	14.2	$\frac{g_{12}}{RT_0} = 6.362 - 4.562\left(\frac{T}{T_0}\right),\ \frac{g_{21}}{RT_0} = -3.745 + 1.786\left(\frac{T}{T_0}\right)$
CSP-SRK-C3-HV1	3.8	10.8	7.1	21.3	1.2	11.3	$\frac{g_{12}}{RT_0} = 6.313 - 4.214\left(\frac{T}{T_0}\right),\ \frac{g_{21}}{RT_0} = -3.779 + 1.568\left(\frac{T}{T_0}\right)$
CSP-SRK-R23-HV1	5.9	8.4	7.1	12.2	2.9	7.5	$\frac{g_{12}}{RT_0} = 6.609 - 5.387\left(\frac{T}{T_0}\right),\ \frac{g_{21}}{RT_0} = -3.935 + 2.358\left(\frac{T}{T_0}\right)$
SRK-HV1-TWU-VS	4.1	5.5	4.8	3.6	2.5	3.1	$\frac{g_{12}}{RT_0} = 5.820 - 2.565\left(\frac{T}{T_0}\right),\ \frac{g_{21}}{RT_0} = -3.339 + 0.1390\left(\frac{T}{T_0}\right)$
PR-HV1	3.5	8.6	5.9	16.3	1.7	9.0	$\frac{g_{12}}{RT_0} = 5.772 - 2.610\left(\frac{T}{T_0}\right),\ \frac{g_{21}}{RT_0} = -3.346 + 0.2419\left(\frac{T}{T_0}\right)$
PR-HV1-TWU	3.5	5.6	4.5	16.3	1.7	9.0	$\frac{g_{12}}{RT_0} = 5.831 - 2.559\left(\frac{T}{T_0}\right),\ \frac{g_{21}}{RT_0} = -3.311 + 0.03770\left(\frac{T}{T_0}\right)$
PR-HV1-TWU-VS	3.5	5.6	4.5	3.5	2.2	2.8	$\frac{g_{12}}{RT_0} = 5.831 - 2.559\left(\frac{T}{T_0}\right),\ \frac{g_{21}}{RT_0} = -3.311 + 0.03770\left(\frac{T}{T_0}\right)$
Multiparameter EoS							
GERG-2008	85.2	9.8	50.3	2.1	0.6	1.3	–
EoS-CG	9.3	6.5	8.0	0.6	–	–	–

Huron–Vidal mixing rule has a temperature-dependence that has been thoroughly validated by the scientific community. Interestingly, we note that although PC-SAFT-02B is the most accurate association EoS in terms of solubilities, it is the worst in terms of densities; PC-SAFT-04C is the most accurate association EoS for density predictions.

Interestingly, using the 0 scheme for CO_2 and the 2B scheme for H_2O in PC-SAFT yields accurate solubility predictions, but using the same schemes for CPA does not. Indeed, it appears that the best choice of scheme for each of CO_2 and H_2O depends both on the application and the choice of association EoS. For instance, it is generally accepted that CO_2 should be modeled as non-associating when in a hydrocarbon mixture. However, if CO_2 is modeled as non-associating in the CO_2/H_2O system, neither CPA-SRK nor CPA-PR are able to describe the increased H_2O solubility in the CO_2-rich liquid phase compared to the vapor phase [80,90]; PC-SAFT-02B, on the other hand, *is* able to describe it. Tsivintzelis et al. [80] speculates that this is due to a cancellation of errors in PC-SAFT-02B. Previous works [8,90] have shown that for the CPA-PR EoS, the best results are obtained when CO_2 is modeled as a self- and cross-associating molecule; this stands in contrast to the results with CPA-SRK, which performs best when only cross-association (i.e. solvation) is allowed, cf. Table 5.

The pure-component parameters in CPA and PC-SAFT are usually fitted to saturation pressures and liquid densities, and for self-associating components they generally yield [91] more accurate densities than cubic EoS. However, this comes at the expense of not being capable of reproducing the critical temperature and pressure

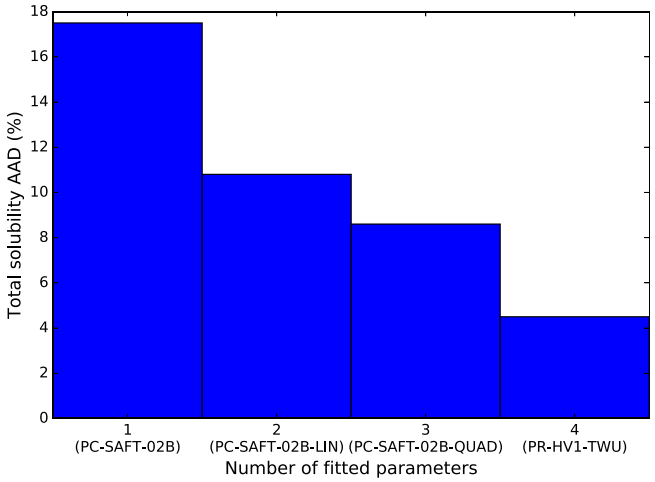

Fig. 5. The bar chart presents the total solubility AAD for the most accurate EoS from Table 5 with a given number of fitting parameters. The most accurate thermodynamic model is indicated in parentheses.

of the fluid, and results in an inconsistent representation of the region near the critical point. This problem has been discussed in the literature [92,93].

4.2.2. The extrapolation behavior

We shall next evaluate the ability of the models to predict data outside the temperature and pressure range used to fit their mixing rules. Instead of fitting excessively many parameters to unvalidated data measured at extreme temperatures and pressures, it may be better to fit fewer parameters to more reliable data, and then extrapolate to regions where reliable measurements are scarce. A priori, one would expect that such an approach is more sound when using a first-principles model such as PC-SAFT. To test this, we computed solubility and density AADs for the models using data outside of the fitting range. For solubilities, we used the aqueous phase data by Guo et al. [20], and CO_2-rich phase data from Tabasinejad et al. [8], but included only the data for which the temperature exceeded 478 K or the pressure exceeded 61 MPa. Results for selected models are given in Table 6.

Table 6
Accuracy of extrapolations for selected models. We compared against 52 (T,P) points for the CO_2 solubility in the range 293 – 573 K, 10 – 120 MPa, and 12 (T,P) points for the H_2O solubility in the range 423 – 478 K, 71 – 129 MPa. Density AADs were computed over the union of two uniform 5×5 grids in *TP*-space: (1) 285 – 478 K and 65 – 120 MPa, (2) 478 – 573 K and 10 – 120 MPa. Reference densities are computed from Hu et al.'s model (ρ_x) and EoS-CG (ρ_y).

Model	x	y	ρ_x	ρ_y
VTPR	11.6	96.8	6.8	3.5
CPA-SRK-04C	15.6	55.6	0.7	2.7
PC-SAFT-04C	14.6	50.2	1.6	1.6
PC-SAFT-02B	21.6	67.4	6.4	1.1
PC-SAFT-02B-ORD2	11.9	48.1	6.5	0.9
PR-WS-TWU	21.3	88.6	17.1	12.7
CPA-SRK-S4C	18.6	46.3	0.8	2.9
CSP-SRK-C1-HV1	6.8	9.2	25.6	4.9
CSP-SRK-C3-HV1	7.0	4.7	22.2	3.4
PR-HV1-TWU-VS	5.6	12.7	6.8	1.7
EoS-CG	14.8	10.1	2.0	–

Fig. 6 illustrates how the densities computed from PR-HV1-TWU-VS and CPA-SRK-04C compare with the reference densities provided by EoS-CG. In the aqueous phase, CPA-SRK-04C is very accurate, while PR-HV1-TWU-VS performs poorly even with the volume shift. In the CO_2-rich phase, the density predictions of PR-HV1-TWU-VS are closer to the reference densities (from EoS-CG) than CPA-SRK-04C, especially at high temperatures and pressures; however, there does not exist any density measurements of the CO_2-rich phase at these extreme conditions, and EoS-CG is also extrapolated here. The density extrapolations of both examined EoS have the correct trend, i.e the partial derivatives of $\rho(T,P)$ have the correct sign and comparable magnitudes.

Table 6 shows that the CSP-HV1 models have by far the best extrapolative abilities for the solubilities. PR-HV1-TWU-VS, which is the best model for predicting solubilities in the fitting region, yields poor solubility extrapolations in the CO_2-rich phase. Indeed, Fig. 7b shows that PR-HV1-TWU-VS incorrectly predicts that the solubility of H_2O in the CO_2-rich phase decreases with pressure. The

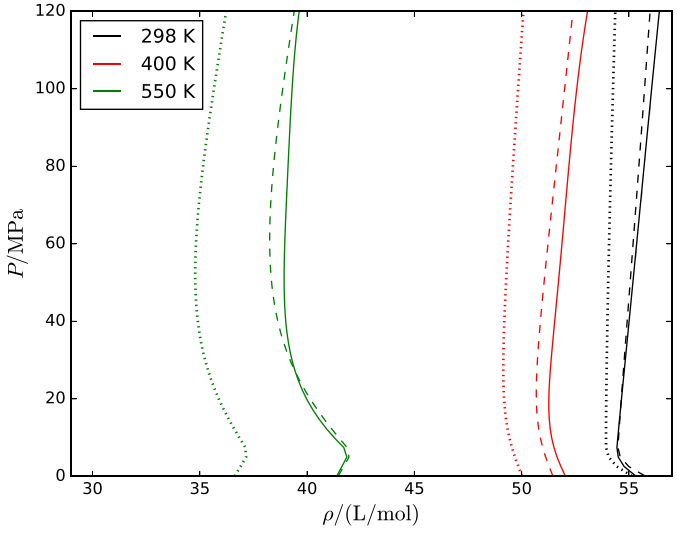

(a) Density of aqueous phase.

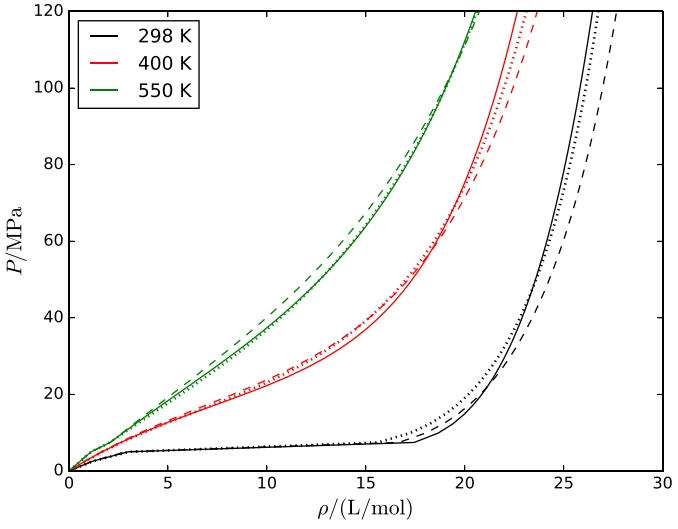

(b) Density of CO_2-rich phase.

Fig. 6. Densities as computed from CPA-SRK-04C (dashed curve), PR-HV1-TWU-VS (dotted curve) and reference model (solid curve). The reference model for the aqueous is the correlation by Hu et al. [34], while EoS-CG is the reference model for the CO_2-rich phase. Densities have been computed at saturation compositions, as calculated by EoS-CG. The kink at 298 K in Fig. 6b is due to the transition from VLE to LLE.

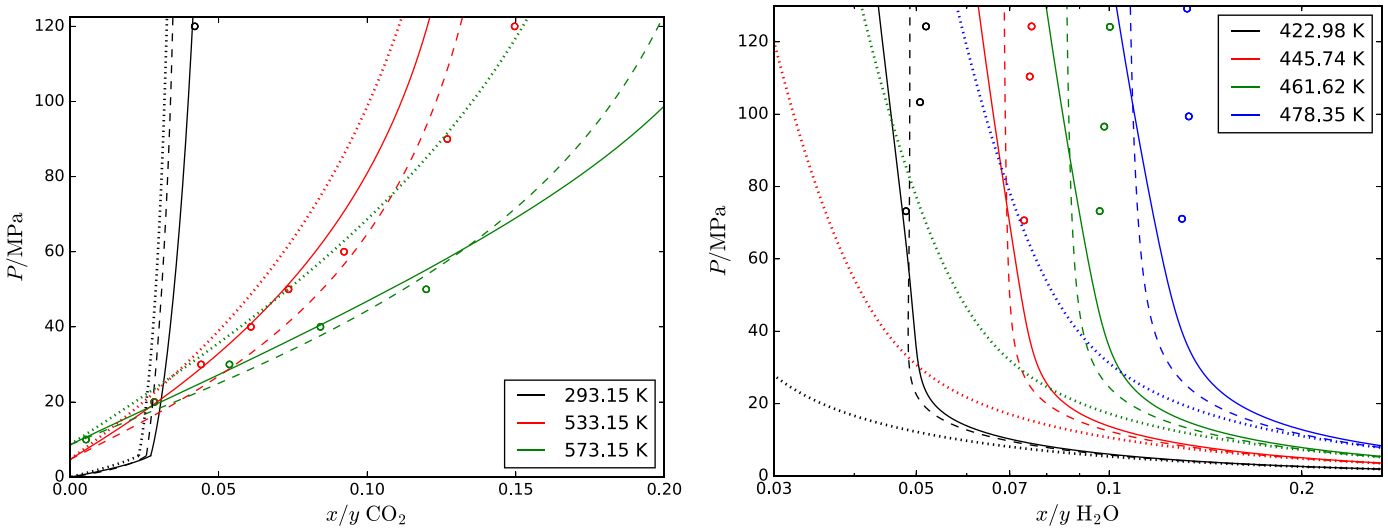

(a) Solubility of CO_2 in the aqueous phase. Data: Guo et al. [20].

(b) Solubility of H_2O in the CO_2-rich phase. Data: Tabasinejad et al. [8].

Fig. 7. Extrapolation of solubilities outside the region of fitting. PR-HV1-TWU (solid curve), EoS-CG (dashed curve), and CPA-SRK-04C (dotted curve). The kink at 293.15 K in Fig.7a is due to the transition from VLE to LLE.

model which uses the Wong–Sandler mixing rules also extrapolates very poorly for the CO_2-rich phase, even though Table 5 shows that it reproduces the CO_2-rich phase data used for fitting well. Almost all the extrapolated models give a more accurate CO_2 solubility than H_2O solubility. This may mean that the high-pressure CO_2-rich phase data by Tabasinejad et al. [8] are inaccurate, or that it simply is more difficult to predict.

4.2.3. A discussion of previous modeling approaches

It is important to discuss the present work in light of previous modeling efforts aiming to accurately represent the *PVTxy* behavior of CO_2/H_2O mixtures. Zhao and Lvov [94] evaluated a model for the CO_2/H_2O-system similar to the Huron–Vidal mixing rule used here, by incorporating an NRTL-like temperature dependence into the Wong–Sandler mixing rule, in addition to a first-order composition dependence for the binary interaction parameter. Such a model is likely to be just as successful as the Huron–Vidal mixing rule, and it is physically more correct in the sense that it gives the theoretically correct composition dependence of the second virial coefficient. Some of the data used in the fitting process by Zhao and Lvov are of questionable quality, e.g. the LLE data by Hou et al. [16]. In the fitting process, four parameters per temperature were used, whereas the best model in our study (PR-HV1-TWU-VS) uses four parameters in total. Hence, their model would be easier to use if a temperature correlation simpler than cubic splines were developed.

Tsivintzelis et al. [80] concluded that CPA-SRK is a good model for the CO_2/H_2O system if the 4C scheme is used for water and CO_2 is modeled as solvating, a conclusion supported by Table 5. The concept of solvation was implemented, as in this work, by modeling CO_2 as having sites all of the same polarity, with a corresponding association strength ε and an association volume κ. However, a problem with the solvation approach arises if CO_2 is in a mixture where it solvates with more than one molecule. Indeed, examining the results by Tsivintzelis et al. [80], the values of the association strength and association volume of CO_2's association site(s) are seen to depend on the component CO_2 is interacting with. With the current model for solvation, ε and κ thus lose their physical significance as pure-component parameters, and instead become fittable binary interaction parameters. It is thus not clear whether the improved accuracy of the solvation approach is due to a physically more correct model, or the result of including more fitting parameters. Indeed, both CPA-PR and PC-SAFT are capable of representing the CO_2/H_2O mixture to a good accuracy without using the solvation approach. However, although certain features of CPA sometimes appear more like correlations than physical models, in practice it has proven enormously successful in reproducing the behavior of complex mixtures [41,95,96].

Tang and Gross [83] modeled phase equilibria of various mixtures containing acid gases with both PC-SAFT and PCP-SAFT, showing that PCP-SAFT offers systematic improvements compared to PC-SAFT. The CO_2/H_2O system was modeled with PCP-SAFT (but not PC-SAFT), and they used a quadratic temperature dependence of the k_{ij} parameter. In other words, their model corresponds to PCP-SAFT-02B-ORD2 in Table 5, the only difference being that we use simplified mixing rules; that this difference is insignificant is indicated by the fact that our fit of PCP-SAFT-02B-ORD2 gave optimal parameters very close to the ones found in 83. From Table 5 we draw the conclusion that modeling the quadrupolar moment of CO_2 does not improve the fit for the CO_2/H_2O system. This possibly stems from the interdependence of associating interactions and dipolar interaction not being accounted for, seeing as the dipole moment of water is not explicitly modeled. Tang and Gross [83] outlined a remedy to this problem: to choose a dipolar reference fluid in the association theory underpinning the PCP-SAFT model. To the best of our knowledge, this approach has not yet been realized within the PC-SAFT framework.

Tang and Gross [83] also present a modified mixing rule for the dispersive term in PCP-SAFT, utilizing an extra, asymmetric binary interaction parameter l_{ij}, yielding improved results on the binary system H_2S/CH_4. Considering the success of the asymmetric Huron–Vidal mixing rule demonstrated in Table 5, implementing such an approach has the potential to lower the AAD of the fit. However, the modified mixing rule is not given a physical interpretation, and one can thus question what its benefits are compared to a physically sound approach such as e.g. explicitly modeling the octapole moment of CH_4.

Austegard et al. [89] fitted an SRK-HV2 model and obtained an

AAD of 2.6% for the solubility of CO_2 in H_2O and 7.4% for H_2O in CO_2. In addition to using less and older data than this work, the data that deviated substantially from the model were not included when computing the AAD. For applications below 61 MPa and 478 K, we recommend using the parameters presented in Table 5 for accurate representation of the CO_2/H_2O -mixture with Huron–Vidal mixing rules.

The SAFT-LJ EoS by Sun and Dubessy [91] is another EoS from the SAFT family that uses the Lennard-Jones intermolecular potential to describe dispersion interactions. All terms have physical meaning. In addition to accounting for the self-association of H_2O, it explicitly accounts for both the quadrupole moment of CO_2 and the dipole moment of H_2O. It is able to correlate the CO_2/H_2O solubility behavior well, but is extremely complex and computationally intensive, and needs improvised correlations for interaction parameters. The model may need to be re-fitted, as some measurements they have used in the fitting process (e.g. dew point data by Tödheide and Franck [87]) are of questionable accuracy.

5. Conclusion

This work presented a comprehensive comparison of a wide selection of thermodynamic models for describing the *PVTxy* behavior, i.e. the densities and the phase compositions, of CO_2/H_2O -mixtures. All thermodynamic models were fitted to the same experimental data and compared on the same basis. This allowed us to make rather general statements.

First, the most accurate experimental data were identified in the temperature range 273–478 K and for pressures below 61 MPa, by conducting a critical, up-to-date literature survey. The literature survey revealed that the phase behavior of water saturated with CO_2 is well-characterized experimentally, both when it comes to CO_2 concentration and densities. For the CO_2-rich phases however, we identified temperature and pressure ranges where accurate measurements are needed, both with respect to densities and phase compositions.

The most reliable data were next used to fit the binary interaction parameters of a wide range of thermodynamic models: cubic equations of state (EoS) with quadratic/Wong–Sandler/Huron–Vidal mixing rules, PC-SAFT, PCP-SAFT and CPA with different association schemes, and corresponding states models with various reference fluids. The predictive ability of the models was tested by comparing to data outside of the *TP* region used in the parameter-fit. We discussed strengths and weaknesses of the thermodynamic models. The multiparameter EoS-CG, PC-SAFT, and cubic EoS with Huron–Vidal mixing rules and volume shift, were found to represent the experimental data most accurately.

The association EoS outperformed cubic EoS when only a few binary interaction parameters were used, but the flexibility of the Huron–Vidal mixing rule in representing solubility behavior was apparent when enough parameters were employed. The association EoS were capable of better density predictions than cubic EoS, even when applying a volume shift to the latter. The corresponding states approaches we tested performed on-par with cubic EoS without volume shifts, but had better extrapolation abilities. One drawback of association EoS compared to the other EoS is that they misrepresent the critical region of pure components, a deficiency that carries over to mixtures.

At least three fitting parameters were needed to represent the *PVTxy* behavior of CO_2/H_2O mixtures within an accuracy of 10%, where PC-SAFT with the 2B association scheme for water was most accurate for representing the solubility. By including a fourth parameter, it was possible to improve the accuracy in the prediction of phase compositions, where the Peng–Robinson cubic EoS with Huron–Vidal mixing rules and volume shift gave the best results with an average accuracy of 4.5% and 2.8% for predicting phase compositions and densities respectively. However, this model gave the incorrect trend for the solubility when extrapolated to extreme pressures in the CO_2-rich phase. The most accurate multiparameter EoS, EoS-CG, exhibited an average accuracy of 8.0% and 0.6% for predicting phase compositions and aqueous densities respectively.

Acknowledgements

The research leading to these results has received funding from the Norwegian Financial Mechanism 2009-2014 under Project Contract no. 7F14466. The authors also thank the HYVA project for support, and they are grateful to Sara Febra and the anonymous reviewers for helpful comments.

References

[1] S. Bachu, J. Adams, Sequestration of CO_2 in geological media in response to climate change: capacity of deep saline aquifers to sequester CO_2 in solution, Energy Convers. Manage 44 (20) (2003) 3151–3175, http://dx.doi.org/10.1016/S0196-8904(03)00101-8.

[2] R. M. Enick, S. M. Klara, Effects of CO_2 solubility in brine on the compositional simulation of CO_2 floods, SPE Reserv. Eng. 7(2), doi:10.2118/20278-PA.

[3] A. Chapoy, R. Burgass, B. Tohidi, I. Alsiyabi, Hydrate and phase behavior modeling in CO_2-rich pipelines, J. Chem. Eng. Data 60 (2) (2015) 447–453, http://dx.doi.org/10.1021/je500834t.

[4] H. Nagashima, N. Fukushima, R. Ohmura, Phase equilibrium condition measurements in carbon dioxide clathrate hydrate forming system from 199.1 K to 247.1 K, J. Chem. Eng. Data 413 (2016) 53–56, http://dx.doi.org/10.1016/j.fluid.2015.09.020.

[5] J.O. Valderrama, C.A. Faúndez, Thermodynamic consistency test of high pressure gas-liquid equilibrium data including both phases, Thermochim. Acta 499 (2010) 85–90, http://dx.doi.org/10.1016/j.tca.2009.11.006.

[6] N. Spycher, K. Pruess, J. Ennis-King, CO_2-H_2O mixtures in the geological sequestration of CO_2. I. Assessment and calculation of mutual solubilities from 12 to 100 C and up to 600 bar, Geochim. Cosmochim. Ac 67 (2003) 3015–3031, http://dx.doi.org/10.1016/S0016-7037(03)00273-4.

[7] L. Diamond, N. Akinfiev, Solubility of CO_2 in water from -1.5 to 100 C to 100 MPa: evaluation of literature data and thermodynamic modelling, Fluid Phase Equilib. 208 (2003) 265–290, http://dx.doi.org/10.1016/S0378-3812(03)00041-4.

[8] F. Tabasinejad, R. Moore, S. Mehta, K.V. Fraassen, Y. Barzin, J. Rushing, K. Newsham, Water solubility in supercritical methane, nitrogen, and carbon dioxide: measurement and modeling from 422 to 483 K and pressures from 3.6 to 134 MPa, Ind. Eng. Chem. Res. 50 (2011) 4029–4041, http://dx.doi.org/10.1021/ie101218k.

[9] R. Capobianco, M. S. Gruskiewicz, D. J. Wesolowski, D. R. Cole, R. J. Bodnar, Columetric properties and fluid phase equilibria of CO_2+H_2O, in: Thirty-Eight Workshop on Geothermal Reservoir Engineering, Stanford, USA, 1–8, 2013.

[10] Z. Duan, R. Sun, An improved model calculating CO_2 solubility in pure water and aqueous NaCl solution from 273 to 533 K and from 0 to 2000 bar, Chem. Geol. 193 (2003) 257–271, http://dx.doi.org/10.1016/S0009-2541(02)00263-2.

[11] A. Valtz, A. Chapoy, C. Coquelet, P. Paricaud, D. Richon, Vapour-liquid equilibria in the carbon dioxide-water system, measurement and modelling from 278.2 to 318.2 K, Fluid Phase Equilib. 226 (2004) 333–344, http://dx.doi.org/10.1016/j.fluid.2004.10.013.

[12] M. Bermejo, A. Martin, L. Florusse, C. Peters, M. Cocero, The influence of Na_2SO_4 on the CO_2 solubility in water at high pressure, Fluid Phase Equilib. 238 (2005) 220–228, http://dx.doi.org/10.1016/j.fluid.2005.10.006.

[13] D. Koschel, J. Coxam, L. Rodier, V. Majer, Enthalpy and solubility data of CO_2 in water and NaCl(aq) at conditions of interest for geological sequestration, Fluid Phase Equilib. 247 (2006) 107–129, http://dx.doi.org/10.1016/j.fluid.2006.06.006.

[14] X. Han, Z. Yu, T. Qi, W. Guo, G. Zhang, Measurement and correlation of solubility data for CO_2 in Na_2HCO_3 aqueous solution, J. Chem. Eng. Data 56 (2011) 1213–1219, http://dx.doi.org/10.1021/je1011168.

[15] F. Lucile, P. Cezac, F. Contamine, J. Serin, D. Houssin, P. Arpentier, Solubility of carbon dioxide in water and aqueous solution containin sodium hydrocide at temperature from (293.15 to 393.15) K and pressure up to 5 MPa: experimental measurements, J. Chem. Eng. Data 57 (2012) 784–789, http://dx.doi.org/10.1021/je200991x.

[16] S. Hou, G. Maitland, J. Trusler, Measurement and modeling of the phase behavior of the (carbon dioxide+water) mixture at temperatures from 298.15 to 448.15 K, J. Supercrit. Fluid 73 (2013) 87–96, http://dx.doi.org/10.1016/j.supflu.2012.11.011.

[17] W. Song, H. Fadaei, D. Sinton, Determination of dew point conditions for CO_2 with impurities using microfluidics, Envir. Sci. Tech. 48 (2014) 3567–3574, http://dx.doi.org/10.1021/es404618y.

[18] C. Jiang, J. Wu, Z. Sun, Q. Pan, Solubility of water in supercritical CO_2, Huaxue

Gongcheng 42 (2014) 42–47 doi:0.3969/j.issn.http://dx.doi.org/1005-9954.2014.07.009.
[19] C. Meyer, A. Harvey, Dew-point measurements for water in compressed carbon dioxide, AIChE J. 61 (9) (2015) 2913–2925, http://dx.doi.org/10.1002/aic.14818.
[20] H. Guo, Y. Chen, Q. Hu, W. Lu, W. Ou, L. Geng, Quantitative raman spectroscopic measurements of CO_2 solubility in NaCl solution from (273.15 to 473.15) K at p = (10.0, 20.0, 30.0, and 40.0) MPa, J. Chem. Eng. Data 61 (1) (2016) 466–474, http://dx.doi.org/10.1021/acs.jced.5b00651.
[21] S. Foltran, M.E. Vosper, N.B. Suleiman, A. Wriglesworth, J. Ke, T.C. Drage, M. Poliakoff, M.W. George, Understanding the solubility of water in carbon capture and storage mixtures: an FTIR spectroscopic study of H_2O+CO_2+N_2 ternary mixtures, Int. J. Greenh. Gas. Con 35 (2015) 131–137, http://dx.doi.org/10.1016/j.ijggc.2015.02.002.
[22] G. Comak, S. Foltran, J. Ke, E. Perez, Y. Sanchez-Vicente, M. George, M. Poliakoff, A synthetic-dynamic method for water solubility measurements in high pressure CO_2 using ATR-FTIR spectroscopy, J. Chem. Thermodyn. 93 (2016) 386–391, http://dx.doi.org/10.1016/j.jct.2015.09.024.
[23] R. Wiebe, V. Gaddy, The solubility in water of carbon dioxide at 50, 75 and 100 C, at pressures to 700 atmospheres, J. Am. Chem. Soc. 61 (1939) 315–318, http://dx.doi.org/10.1021/ja01871a025.
[24] R. Wiebe, V. Gaddy, The solubility of carbon dioxide in water at various temperatures from 12 to 40 C and at pressures up to 500 atmospheres: critical phenomena, J. Am. Chem. Soc. 62 (1940) 815–817, http://dx.doi.org/10.1021/ja01861a033.
[25] R. Wiebe, V.L. Gaddy, Vapor phase composition of carbon dioxide-water mixtures at various temperatures and at pressures to 700 atmospheres, J. Am. Chem. Soc. 63 (2) (1941) 475–477, http://dx.doi.org/10.1021/ja01847a030.
[26] C. Coan, A. King, Solubility of water in compressed carbon dioxide, nitrous oxide, and ethane. Evidence for hydration of carbon dioxide and nitrous oxide in the gas phase, J. Am. Chem. Soc. 93 (1971) 1857–1862, http://dx.doi.org/10.1021/ja00737a004.
[27] A. Zawisza, B. Malesinska, Solubility of carbon dioxide in liquid water and of water in gaseous carbon dioxide in the range 0.2-5 MPa and at temperatures up to 473 K, J. Chem. Eng. Data 26 (4) (1981) 388–391, http://dx.doi.org/10.1021/je00026a012.
[28] T. Nakayama, H. Sagara, K. Arai, S. Saito, High pressure liquid-liquid equilibria for the system of water, ethanol and 1,1-difluoroethane at 323.2 K, Fluid Phase Equilib. 38 (1987) 109–127, http://dx.doi.org/10.1016/0378-3812(87)90007-0.
[29] J. Briones, J. Mullins, M. Thies, B. Kim, Ternary phase equilibria for acetic acid-water mixtures with supercritical carbon dioxide, Fluid Phase Equilib. 36 (1987) 235–246, http://dx.doi.org/10.1016/0378-3812(87)85026-4.
[30] G. Müller, E. Bender, G. Maurer, Das Dampf-Flüssigkeitsgleichgewicht des ternären Systems Ammoniak-Kohlendioxid-Wasser bei hohen Wassergehalten im Bereich zwischen 373 und 473 Kelvin, Ber. Bunsenges. Phys. Chem. 92 (1988) 148–160, http://dx.doi.org/10.1002/bbpc.198800036.
[31] M. King, A. Mubarak, J. Kim, T. Bott, The mutual solubilities of water with supercritical and liquid carbon dioxide, J. Supercrit. Fluid 5 (1992) 296–302, http://dx.doi.org/10.1016/0896-8446(92)90021-B.
[32] A. Bamberger, G. Sieder, G. Maurer, High-pressure (vapor+liquid) equilibrium in binary mixtures of (carbon dioxide+water or acetic acid) at temperatures from 313 to 353 K, J. Supercrit. Fluid 17 (2000) 97–110, http://dx.doi.org/10.1016/S0896-8446(99)00054-6.
[33] G. Anderson, Solubility of carbon dioxide in water under incipient clathrate formation conditions, J. Chem. Eng. Data 47 (2002) 219–222, http://dx.doi.org/10.1021/je015518c.
[34] Q. Hu, H. Guo, X. Lü, Q. Lu, Y. Chen, Y. Zhu, L. Geng, Determination of P-V-T-x properties of the CO_2-H_2O system up to 573.15 K and 120 MPa - experiments and model, Chem. Geol. 424 (2016) 60–72, http://dx.doi.org/10.1016/j.chemgeo.2016.01.011.
[35] H. Teng, A. Yamasaki, M.-K. Chun, H. Lee, Solubility of liquid CO_2 in water at temperatures from 278 to 293 K and pressures from 6.44 MPa ato 29.49 MPa and densities of the corresponding aqueous solutions, J. Chem. Thermodyn. 29 (1997) 1301–1310, http://dx.doi.org/10.1006/jcht.1997.0249.
[36] J. Gernert, R. Span, EOS-CG: a Helmholtz energy mixture model for humid gases and CCS mixtures, J. Chem. Thermodyn. 93 (2016) 274–293, http://dx.doi.org/10.1016/j.jct.2015.05.015.
[37] A. Hebach, A. Oberhof, N. Dahmen, Density of water + carbon dioxide at elevated pressures: measurements and correlation, J. Chem. Eng. Data 49 (4) (2004) 950–953, http://dx.doi.org/10.1021/je034260i.
[38] M. Wendland, H. Hasse, G. Maurer, Experimental pressure-temperature data on three- and four-phase equilibria of fluid, hydrate, and ice phases in the system carbon dioxide-water, J. Chem. Eng. Data 44 (1999) 901–906, http://dx.doi.org/10.1021/je980208o.
[39] P. H. v. Konynenburg, R.L. Scott, Critical lines and phase equilibria in binary van der Waals mixtures, Philos. Trans. R. Soc. Lond. A 298 (1980) 495–540.
[40] H. Li, J.P. Jakobsen, Ø. Wilhelmsen, J. Yan, PVTxy properties of CO_2 mixtures relevant for CO_2 capture, transport and storage: review of available experimental data and theoretical models, Appl. Energ 88 (11) (2011) 3567–3579, http://dx.doi.org/10.1016/j.apenergy.2011.03.052.
[41] G.M. Kontogeorgis, G. Folas, Thermodynamic Models for Industrial Applications, Wiley, 2010, http://dx.doi.org/10.1002/9780470747537.
[42] D.Y. Peng, D.B. Robinson, A new two-constant equation of state, Ind. Eng. Chem. Fund. 15 (1) (1976) 59–64, http://dx.doi.org/10.1021/i160057a011.
[43] G. Soave, Equilibrium constants from a modified Redlich-Kwong equation of state, Chem. Eng. Sci. 27 (6) (1972) 1197–1203, http://dx.doi.org/10.1016/0009-2509(72)80096-4.
[44] M.L. Michelsen, J.M. Mollerup, Thermodynamic Models: Fundamentals & Computational Aspects, second ed., Tie-Line Publications, Holte, Denmark, 2007, ISBN 87-989961-3-4.
[45] A. Péneloux, E. Rauzy, R. Fréze, A consistent correction for Redlich-Kwong-Soave volumes, Fluid Phase Equilib. 8 (1) (1982) 7–23, http://dx.doi.org/10.1016/0378-3812(82)80002-2.
[46] B.S. Jhaveri, G.K. Youngren, Three-parameter modification of the peng-robinson equation of state to improve volumetric predictions, SPE Reserv. Eng. 8 (1988) 1033–1040, http://dx.doi.org/10.2118/13118-PA.
[47] C.H. Twu, D. Bluck, J.R. Cunningham, J.E. Coon, A cubic equation of state with a new alpha function and a new mixing rule, Fluid Phase Equilib. 69 (1991) 33–50, http://dx.doi.org/10.1016/0378-3812(91)90024-2.
[48] M.-J. Huron, J. Vidal, New mixing rules in simple equations of state for representing vapour-liquid equilibria of strongly non-ideal mixtures, Fluid Phase Equilib. 3 (4) (1979) 255–271, http://dx.doi.org/10.1016/0378-3812(79)80001-1.
[49] M.L. Michelsen, A modified Huron-Vidal mixing rule for cubic equations of state, Fluid Phase Equilib. 60 (1) (1990) 213–219, http://dx.doi.org/10.1016/0378-3812(90)85053-D.
[50] S.F. Westman, H.J. Stang, S.W. Løvseth, A. Austegard, I. Snustad, S.Ø. Størset, I.S. Ertesvåg, Vapor-liquid equilibrium data for the carbon dioxide and nitrogen (CO_2+N_2) system at the temperatures 223, 270, 298 and 303 K and pressures up to 18 MPa, Fluid Phase Equilib. 409 (2016) 207–241, http://dx.doi.org/10.1016/j.fluid.2015.09.034.
[51] S.F. Westman, H.J. Stang, S.W. Løvseth, A. Austegard, I. Snustad, S.Ø. Størset, I.S. Ertesvåg, Vapor-liquid equilibrium data for the carbon dioxide and oxygen (CO_2+O_2) system at the temperatures 218, 233, 253, 273, 288 and 298 K and pressures up to 14 MPa, Fluid Phase Equilib. 421 (2016) 67–87, http://dx.doi.org/10.1016/j.fluid.2016.04.002.
[52] A. Fredenslund, R.L. Jones, J.M. Prausnitz, Group-contribution estimation of activity coefficients in nonideal liquid mixtures, AIChE J. 21 (6) (1975) 1086–1099, http://dx.doi.org/10.1002/aic.690210607.
[53] D.S. Abrams, J.M. Prausnitz, Statistical thermodynamics of liquid mixtures: a new expression for the excess Gibbs energy of partly or completely miscible systems, AIChE J. ISSN: 1547-5905 21 (1) (1975) 116–128, http://dx.doi.org/10.1002/aic.690210115.
[54] J.P. Flory, Thermodynamics of high polymer solutions, J. Chem. Phys. 9 (1941) 660–661, http://dx.doi.org/10.1063/1.1750971.
[55] M.L. Huggins, Solution of long chain compounds, J. Phys. Chem. 9 (1941) 440, http://dx.doi.org/10.1063/1.1750930.
[56] E.A. Guggenheim, Mixtures: the Theory of the Equlibrium Properties of Some Simple Classes of Mixtures Solutions and Alloys, the International Series of Monographs on Physics, Clarendon Press, Oxford, UK, 1952.
[57] T. Holderbaum, J. Gmehling, PSRK: a group contribution equation of state based on UNIFAC, Fluid Phase Equilib. 70 (2–3) (1991) 251–265, http://dx.doi.org/10.1016/0378-3812(91)85038-V.
[58] E. Collinet, J. Gmehling, Prediction of phase equilibria with strong electrolytes with the help of the volume translated Peng-Robinson group contribution equation of state (VTPR), Fluid Phase Equilib. 246 (1–2) (2006) 111–118, http://dx.doi.org/10.1016/j.fluid.2006.05.033.
[59] E. Voutsas, K. Magoulas, D. Tassios, Universal mixing rule for cubic equations of state applicable to symmetric and asymmetric systems: results with the peng-robinson equation of state, Ind. Eng. Chem. Res. 43 (19) (2004) 6238–6246, http://dx.doi.org/10.1021/ie049580p.
[60] K. Magoulas, D. Tassios, Thermophysical properties of n-Alkanes from C1 to C20 and their prediction for higher ones, Fluid Phase Equilib. 56 (1990) 119–140, http://dx.doi.org/10.1016/0378-3812(90)85098-U.
[61] G. Avlonitis, G. Mourikas, S. Stamataki, D. Tassios, A generalized correlation for the interaction coefficients of nitrogen-hydrocarbon binary mixtures, Fluid Phase Equilib. 101 (1994) 53–68, http://dx.doi.org/10.1016/0378-3812(94)02554-1.
[62] B. Schmid, A. Schedemann, J. Gmehling, Extension of the VTPR group contribution equation of state: group interaction parameters for additional 192 group combinations and typical results, Ind. Eng. Chem. Res. 53 (8) (2014) 3393–3405, http://dx.doi.org/10.1021/ie404118f.
[63] H.K. Hansen, P. Rasmussen, A. Fredenslund, M. Schiller, J. Gmehling, Vapor-liquid equilibria by UNIFAC group contribution. 5. Revision and extension, Ind. Eng. Chem. Res. 30 (10) (1991) 2352–2355, http://dx.doi.org/10.1021/ie00058a017.
[64] R. Wittig, J. Lohmann, J. Gmehling, Vapor-liquid equilibria by UNIFAC group contribution. 6. Revision and extension, Ind. Eng. Chem. Res. 42 (1) (2003) 183–188, http://dx.doi.org/10.1021/ie020506l.
[65] D.S.H. Wong, S.I. Sandler, A theoretically correct mixing rule for cubic equations of state, AIChE J. 38 (5) (1992) 671–680, http://dx.doi.org/10.1002/aic.690380505.
[66] H. Renon, J.M. Prausnitz, Local compositions in thermodynamic excess functions for liquid mixtures, AIChE J. 14 (1) (1968) 135–144, http://dx.doi.org/10.1002/aic.690140124.
[67] O. Jørstad, Equations of State for Hydrocarbon Mixtures, Dissertation, Norwegian Institute of Technology (NTH), 1993.
[68] Ø. Wilhelmsen, G. Skaugen, O. Jørstad, H. Li, Evaluation of SPUNG and other

Equations of State for use in Carbon Capture and Storage modelling, in: N. A. Røkke, M.-B. Hägg, M. J. Mazzetti (Eds.), 6th Trondheim Conference on CO_2 Capture, Transport and Storage (TCCS-6), BIGCCS/SINTEF/NTNU, Energy Procedia vol. 23, Trondheim, Norway, 236–245, doi: http://dx.doi.org/10.1016/j.egypro.2012.06.024, 2012.
[69] M. Ibrahim, G. Skaugen, I. Ertesvåg, An extended corresponding states equation of state (EOS) for CCS industry, Chem. Eng. Sci. 137 (2015) 572–582, http://dx.doi.org/10.1016/j.ces.2015.06.013.
[70] B.A. Younglove, J.F. Ely, Thermophysical properties of fluids. II. Methane, ethane, propane, isobutane, and normal butane, J. Phys. Chem. Ref. Data 16 (4) (1987) 577–798, http://dx.doi.org/10.1063/1.555785.
[71] A. Polt, Zur Beschreibung der thermodynamischen Eigenschaften reiner Fluide mit erweiterter BWR-Gleichungen, Dissertation, Kaiserslautern, 1986.
[72] G.M. Kontogeorgis, E.C. Voutsas, I.V. Yakoumis, D.P. Tassios, An equation of state for associating fluids, Ind. Eng. Chem. Res. 35 (11) (1996) 4310–4318, http://dx.doi.org/10.1021/ie9600203.
[73] J. Gross, G. Sadowski, Perturbed-chain SAFT: an equation of state based on a perturbation theory for chain molecules, Ind. Eng. Chem. Res. 40 (4) (2001) 1244–1260, http://dx.doi.org/10.1021/ie0003887.
[74] J. Gross, An equation-of-state contribution for polar components: quadrupolar molecules, AIChE J. 51 (9) (2005) 2556–2568, http://dx.doi.org/10.1002/aic.10502.
[75] J. Gross, J. Vrabec, An equation-of-state contribution for polar components: dipolar molecules, AIChE J. 52 (3) (2006) 1194–1204, http://dx.doi.org/10.1002/aic.10683.
[76] J. Vrabec, J. Gross, Vapor-liquid equilibria simulation and an equation of state contribution for dipole-quadrupole interactions, J. Phys. Chem. B 112 (1) (2008) 51–60, http://dx.doi.org/10.1021/jp072619u.
[77] G. M. Kontogeorgis, I. V. Yakoumis, H. Meijer, E. Hendriks, T. Moorwood, Multicomponent phase equlibrium calculations for water-methanol-alkane mixtures, Fluid Phase Equilib. 158–160, doi:http://dx.doi.org/10.1016/S0378-3812(99)00060-6.
[78] N. von Solms, M. Michelsen, G. Kontogeorgis, Computational and physical performance of a modified PC-SAFT equation of state for highly asymmetric and associating mixtures, Ind. Eng. Chem. Res. 42 (2003) 1098–1105, http://dx.doi.org/10.1021/ie020753p.
[79] Y. Danten, T. Tassaing, M. Besnard, Ab initio investigation of vibrational spectra of water-$(CO_2)_n$ complexes ($n = 1, 2$), J. Phys. Chem. A 109 (14) (2005) 3250–3256.
[80] I. Tsivintzelis, G.M. Kontogeorgis, M.L. Michelsen, E.H. Stenby, Modeling phase equilibria for acid gas mixtures using the CPA equation of state. Part II: Binary mixtures with CO_2, Fluid Phase Equilib. 306, doi: http://dx.doi.org/10.1016/j.fluid.2011.02.006.
[81] G. Pappa, C. Perakis, I. Tsimpanogiannis, E. Voutsas, Thermodynamic modeling of the vapor-liquid equilibrium of the CO_2/H_2O mixture, Fluid Phase Equilib. 284 (2009) 56–63, http://dx.doi.org/10.1016/j.fluid.2009.06.011.
[82] J. Gross, G. Sadowski, Application of the perturbed-chain SAFT equation of state to associating systems, Ind. Eng. Chem. Res. 41 (22) (2002) 5510–5515, http://dx.doi.org/10.1021/ie010954d.
[83] X. Tang, J. Gross, Modeling the phase equilibria of hydrogen sulfide and carbon dioxide in mixture with hydrocarbons and water using the PCP-SAFT equation of state, Fluid Phase Equilib. 293 (2010) 11–21, http://dx.doi.org/10.1016/j.fluid.2010.02.004.
[84] O. Kunz, W. Wagner, The GERG-2008 wide-range equation of state for natural gases and other mixtures: an expansion of GERG-2004, J. Chem. Eng. Data 57 (11) (2012) 3032–3091, http://dx.doi.org/10.1021/je300655b.
[85] P.T. Boggs, T.H. Byrd, J.E. Rogers, R.B. Schnabel, User's Reference Guide for ODRPACK Version 2.01, Tech. Rep. NISTIR 4834, National Institute of Standards and Technology, 1992.
[86] S. Takenouchi, G. Kennedy, The binary system H_2O-CO_2 at high temperatures and pressures, Am. J. Sci. 262 (9) (1964) 1055–1074, http://dx.doi.org/10.2475/ajs.262.9.1055.
[87] K. Tödheide, E. Franck, Das Zweiphasengebiet und die kritische Kurve im System Kohlendioxid-Wasser bis zu Drucken von 3500 bar, Z. Phys. Chem. 37 (1964) 387–401, http://dx.doi.org/10.1524/zpch.1963.37.5_6.387.
[88] P.C. Gillespie, G.M. Wilson, Vapor-liquid and Liquid-liquid equilibria: Water–methane, Water–carbon dioxide, Water–hydrogen sulfide, Water–n-pentane, Water-methane–n-pentane, Tech. Rep. RR-48, GPA, 1982.
[89] A. Austegard, E. Solbraa, G. De Koeijer, M.J. Mølnvik, Thermodynamic models for calculating mutual solubilities in H_2O-CO_2-CH_4 mixtures, Chem. Eng. Res. Des. 84 (A9) (2006) 781–794, http://dx.doi.org/10.1205/cherd05023.
[90] C. Perakis, E. Voutsas, K. Magoulas, D. Tassios, Thermodynamic modeling of the vapor-liquid equilibiurm of the water/ethanol/CO_2 system, Fluid Phase Equilib. 243 (2006) 142–150, http://dx.doi.org/10.1016/j.fluid.2006.02.018.
[91] R. Sun, J. Dubessy, Prediction of vapor-liquid equilibrium and PVTx properties of geological fluid system with SAFT-LJ EOS including multi-polar contribution. Part I: application to H_2O-CO_2 system, Geochim. Cosmochim. Ac 74 (2010) 1982–1998, http://dx.doi.org/10.1016/j.gca.2010.01.011.
[92] I. Polishuk, Standardized critial point-based numerical solution of statistical association fluid theory parameters: the perturbed chain-statistical association fluid theory equation of state revisited, Ind. Eng. Chem. Res. 53 (2014) 14127–14141, http://dx.doi.org/10.1021/ie502633e.
[93] Ø. Wilhelmsen, A. Aasen, G. Skaugen, P. Aursand, A. Austegard, E. Aursand, M.A. Gjennestad, H. Lund, G. Linga, M. Hammer, Thermodynamic modeling with equations of state: present challenges with established methods, Ind. Eng. Chem. Res. 56 (2017) 3503–3515. http://dx.doi.org/10.1021/acs.iecr.7b00317.
[94] H. Zhao, S.N. Lvov, Phase behavior of the CO_2-H_2O system at temperatures of 273-623 K and pressures of 0.1-200 MPa using Peng-Robinson-Stryjek-Vera equation of state with a modified Wong-Sandler mixing rule: an extension to the CO_2-CH_4-H_2O system, Fluid Phase Equilib. 417 (2016) 96–108, http://dx.doi.org/10.1016/j.fluid.2016.02.027.
[95] G.M. Kontogeorgis, M.L. Michelsen, G.K. Folas, S. Derawi, N. von Solms, E.H. Stenby, Ten years with the CPA (Cubic-Plus-Association) equation of state. Part 1. Pure compounds and self-associating systems, Ind. Eng. Chem. Res. 45 (14) (2006) 4855–4868, http://dx.doi.org/10.1021/ie051305v.
[96] G.M. Kontogeorgis, M.L. Michelsen, G.K. Folas, S. Derawi, N. von Solms, E.H. Stenby, Ten years with the CPA (Cubic-Plus-Association) equation of state. Part 2. Cross-associating and multicomponent systems, Ind. Eng. Chem. Res. 45 (14) (2006) 4869–4878, http://dx.doi.org/10.1021/ie051306n.